Identifying slope processes over time and their imprint in soils of medium-high mountains of Central Europe (the Karkonosze Mountains, Poland)

Waroszewski, Jaroslaw ; Egli, Markus ; Brandová, Dagmar ; Christl, Marcus ; Kabala, Cezary ; Malkiewicz, Malgorzata ; Kierczak, Jakub ; Glina, Bartłomiej ; Jezierski, Paweł

Abstract: Soils in mountainous areas are often polygenetic, developed in slope covers that relate to glacial and periglacial activities of the Pleistocene and Holocene and reflect climatic variations. Landscape development during the Holocene may have been influenced by erosion/solifluction that often started after the Holocene climatic optimum. To trace back soil evolution and its timing, we applied a multi-methodological approach. This approach helped us to outline scenario of soil transformation. According to our results, some aeolian input must have occurred in the late Pleistocene. During that time and the early Holocene, the soils most likely had features of Cryosols or Leptosols. Physico-chemical and mineralogical analyses have indicated that the material was denudated (between late Boreal to the Atlantic) from the ridge and upper slope positions forming a colluvium at midslope positions. Later, during the Sub-Boreal, mass wasting of the remains of silt material deposited at the end of the Pleistocene age on the ridge top seems to have occurred. In addition, the cool and moist conditions caused the deposition of a colluvium at the lower slope positions. The next phase was characterised by the transformation of Leptosols/Cambisols into Podzols at upper slope or shoulder positions and to Albic Cambisols at midslope positions. During the Sub-Boreal period, Stagnosols started to form at the lower part of the slope catena. Overall, the highest erosion rates were calculated at the upper-slope position and the lowest rates at midslope sites. 10Be data showed that the Bs, BC/C were covered during the Holocene by a colluvium with a different geological composition which complicated the calculation of erosion or accumulation rates. The interpretation of erosion and accumulation rates in such multi-layered materials may, therefore, be hampered. However, the multi-methodological reconstruction we applied shed light on the soil and landscape evolution of the eastern Karkonosze Mts.

DOI: https://doi.org/10.1002/esp.4305

Identifying slope processes over time and their imprint in soils of medium-high mountains of Central Europe (the Karkonosze Mountains, Poland)

Jaroslaw Waroszewski[a,1], Markus Egli[b], Dagmar Brandová[b], Marcus Christl[c], Cezary Kabala[a], Malgorzata Malkiewicz[d], Jakub Kierczak[e], Bartłomiej Glina[f], Paweł Jezierski[a]

[a]Institute of Soil Science and Environmental Protection, Wroclaw University of Environmental and Life Sciences, 50-357 Wroclaw, Poland

[b]Department of Geography, University of Zürich, 8057 Zürich, Switzerland

[c]Laboratory of Ion Beam Physics, ETH Zürich, 8093 Zürich, Switzerland

[d]Institute of Geological Sciences, Laboratory of Palynology, University of Wroclaw, 50-205 Wroclaw, Poland

[e]Institute of Geological Sciences, Department of Experimental Petrography, University of Wroclaw, 50-205 Wroclaw, Poland

[f]Poznan University of Life Sciences, Department of Soil Science and Land Protection, Poznan, Poland

Abstract

Soils in mountainous areas are often polygenetic, developed in slope covers that relate to glacial and periglacial activities of the Pleistocene and Holocene and reflect climatic variations. Landscape development during the Holocene may have been influenced by erosion/solifluction that often started after the Holocene climatic optimum. To trace back soil evolution and its timing, we applied a multi-methodological approach. This approach helped us to outline scenario of soil transformation. According to our results, some aeolian input must have occurred in the late Pleistocene. During that time and the early Holocene, the soils most likely had features of Cryosols or Leptosols. Physico-chemical and mineralogical analyses have indicated that the material was denudated (between late Boreal to the Atlantic)

[1]Corresponding author. E-mail address: jaroslaw.waroszewski@upwr.edu.pl (J. Waroszewski)

This article has been accepted for publication and undergone full peer review but has not been through the copyediting, typesetting, pagination and proofreading process which may lead to differences between this version and the Version of Record. Please cite this article as doi: 10.1002/esp.4305

from the ridge and upper slope positions forming a colluvium at midslope positions. Later, during the Sub-Boreal, mass wasting of the remains of silt material deposited at the end of the Pleistocene age on the ridge top seems to have occurred. In addition, the cool and moist conditions caused the deposition of a colluvium at the lower slope positions. The next phase was characterised by the transformation of Leptosols/Cambisols into Podzols at upper slope or shoulder positions and to Albic Cambisols at midslope positions. During the Sub-Boreal period, Stagnosols started to form at the lower part of the slope catena. Overall, the highest erosion rates were calculated at the upper-slope position and the lowest rates at midslope sites. ^{10}Be data showed that the Bs, BC/C were covered during the Holocene by a colluvium with a different geological composition which complicated the calculation of erosion or accumulation rates. The interpretation of erosion and accumulation rates in such multi-layered materials may, therefore, be hampered. However, the multi-methodological reconstruction we applied shed light on the soil and landscape evolution of the eastern Karkonosze Mts.

Key words: soil polygenesis, meteoric ^{10}Be, Pleistocene, landscape evolution, Holocene changes

1. Introduction

The concept of polygenetic soil formation was introduced to soil science a long time ago (Butler, 1959; Yaalon and Ganor, 1973; Huggett, 1975; Simmons, 1978; Gerrard, 1981) and continuously has gained in importance. Nonetheless, multi-layered (stratified) pedons still impose many difficulties for the interpretation of soil genesis and the reconstruction of processes that were responsible for their development (Mailänder and Veit, 2001; Lorz, 2011; Kleber and Terhorst, 2013; Schaetzl and Luehmann, 2013; Waroszewski *et al*., 2013; Migoń and Kacprzak, 2014; Baruck *et al.*, 2016; Waroszewski *et al.*, 2016).

Johnson (1993) and Phillips (2004) indicated that sediment layering and erosion/deposition processes are mainly responsible for texture contrasts and other differences between individual horizons. Johnson (1990, 1993) pointed to the presence of biomantles where slope transport and bioturbation control the thickness of the surface (A horizon) and subsurface horizons (E and B horizons) and soil mixing. Furthermore, soil formation can be sometimes discontinuous over time and has to be conceptualised by 'progressive' or 'regressive' process phases (Johnson and Watson-Steger, 1987; Sommer *et al*., 2008; Waroszewski *et al*., 2016). One morphological feature that testifies soil polygenesis and exposition of the subsoil to the surface and/or climatic oscillations are stone-lines (Johnson, 1990; Eze and Meadows, 2014). So far, 'progressive' or 'regressive' processes were difficult to confirm in mountain soils and, consequently, only in few studies the attempt was made to integrate soil formation, geomorphologic features and sedimentology in a more comprehensive way (e.g. Birkeland *et al*., 2003).

Landscape evolution in the Late Quaternary in the Karkonosze Mountains was strictly controlled by mountain glaciers fluctuations (Engel *et al*., 2010; Engel *et al*., 2013) and intensive erosion (Traczyk and Migoń, 2000). During the last glaciation (Engel *et al*., 2013), periglacial conditions have dominated in the Karkonosze Mountains, with a mean annual

temperature of about -8° to -10°C (Chmal and Traczyk, 1993). During the Holocene period, the cool and moist environmental conditions initiated mass movements on the slopes. The record of such events can be found in postglacial lakes sediments (Chmal and Traczyk, 1998). Malkiewicz *et al*. (2016) correlated the general pedogenetic phases with major climate oscillations, timberline fluctuations, forest succession, rapid deforestation and human impact that were recorded in the lake deposits of Wielki Staw. These records indicated two progressive and two regressive soil evolution phases. It is, however, very difficult to evaluate individual steps of soil evolution because distinct layers with datable organic material (e.g. charcoal), thick aeolian mantles (part of a periglacial cover bed) or tephra substrates are missing. In the Karkonosze Mts. (southern Poland), the age of periglacial sequences is mostly attributed to the Older or Younger Dryas (Waroszewski *et al.*, 2013). Periglacial activities were, however, not only limited to the Pleistocene. Recent studies show that the upper layer of such periglacial cover beds in the Sudetes Mountains may not have been formed during the Pleistocene but also during the Holocene (Waroszewski *et al.*, 2013; Migoń and Kacprzak, 2014; Waroszewski *et al.*, 2015a; Waroszewski *et al.*, 2015b). Consequently, the materials constituting the soil profiles' parent material may have a higher age diversity than previously thought.

Consequently, we hypothesise that soil formation on slopes of the Karkonosze Mountains is not straightforward and demonstrates progressive and regressive trajectories. The processes of soil formation seem to have changed with erosion (mass wasting) and/or accumulation (e.g. due to aeolian input). To address this hypothesis, soil formation and environmental processes need to be evaluated over time. We, therefore, propose a multi-methodological approach that combines pedological, palynological, and mineralogical characteristics and isotope techniques to reconstruct environmental conditions and soil formation on a local scale over this mountainous area. Moreover, soil erosion rates are calculated using a cosmogenic

nuclide (^{10}Be) to trace back the complex evolution of soils within a changing landscape and to propose a model of soil polygenesis.

2. Study area and sampling sites

The study site is situated in the Karkonosze Mountains, a 70 km-long mountain ridge at the border between Poland and the Czech Republic, the central and highest part of the Sudeten Mountains. The Karkonosze Mts. are mostly constituted of Carboniferous granite (two varieties: porphyric and fine-grained) and a Pre-Cambrian/Old-Paleozoic geological unit consisting of such rocks as gneiss, granodiorite, metabasalt, mica schist and hornfels. The Pleistocene sediments are represented by well-preserved moraines which are valuable records of the extent of the different glaciations. Engel *et al.* (2013) dated the Last Glacial Maximum (LGM) and recessional moraines using the radionuclide ^{10}Be and determined their ages between 20.8+/-1.0 and 13.1 +/- 0.5 ka BP (Table 1). The recessional moraines correlated well with the Younger Dryas cold events. Because the exposure ages of moraines of the Łomnica, Łomniczka and Upa Valleys gave an age between 16.2+/-0.7 and 15.5 +/-1.0 ka BP (that seem to correlate to the Oldest Dryas; Engel *et al.*, 2013), we have to assume that the Kowarski Grzbiet area was not ice free before this. The exposure age of the hillslope sediments is, therefore, younger than 16 ka. Post-glacial soil development in the eastern part of Karkonosze Mts. consequently did not start earlier than about 13 to 14 ka ago.

MEAN ANNUAL PRECIPITATION IN THE KARKONOSZE MTS. VARIES PRESENTLY BETWEEN 900 MM AT THE FOOTSLOPE TO 1300 MM IN THE UPPER-MOST PART. MEAN ANNUAL AIR TEMPERATURE RANGES BETWEEN 7 °C AT 600 M A.S.L. AND 1–2 °C AT 1600 M A.S.L., WITH A MINIMUM IN JANUARY-FEBRUARY AND A MAXIMUM IN JULY (ON MT. SNIEZKA −6.1 °C AND 9.4 °C, RESPECTIVELY). SNOW COVER PERSIST THROUGH 200 DAYS DURING THE YEAR ON MT. SNIEZKA. SNOW COVER IS RATHER

shallow on the summit plateau and thicker on the lower slope positions (Sobik et al., 2013). The present study covers a narrow section of the altitude (1142 – 1268 m a.s.l.; Table 2); thus, the climate conditions along the investigated slope vary only very little. The climate, geological and morphological (relief) conditions decide about the vertical zonality of soils in the Karkonosze Mts. The upper zone (above 1400 m a.s.l.) is dominated by *Hyperskeletic/Lithic Leptosols* that developed on a metamorphic/granitic outcrops and block covers having a varying thickness. Between 1200 and 1400 m a.s.l., *Albic Podzols, Stagnic - Histic Podzols* and *Histosols* dominate. Some *Podzols* have inherited the features of cryoturbation and frost action processes. Patterned grounds, mostly inactive, are well preserved here (Kasprzak *et al.*, 2016). In the zone 800-1100 m a.s.l., *Podzols* dominate (Entic, Albic and Histic varieties), but also *Albic Cambisols* and Gleysols greatly contribute. The lowermost slope zone (500 – 800 m a.s.l.) is mostly covered with *Dystric Cambisols* and *Albic Cambisols*, and the footslope and toeslope positions (< 600 m a.s.l.) are dominated by *Luvisols*, developed from fine-grained colluvium (Bojko and Kabala, 2016; Bojko and Kabala *et al.*, 2017; Kabala *et al.*, 2013).

The chosen catena was located in the Kowarski Grzbiet, the easternmost part of the Karkonosze Mts., being a short ridge (4 km) with a narrow nearly flat summit plateau with two peaks: Skalny Stół (1281 m a.s.l.) and Czoło (1266 m a.s.l.). The north-western and south-western slopes of the Kowarski Grzbiet are steep having an inclination of 28 – 44° (Kasprzak and Traczyk, 2013), while the eastern slopes of the ridge are more gentle (10 – 18°). The Kowarski Grzbiet is a remnant of a metamorphic cover of a granite intrusion and is mostly constituted of gneiss, mica schist, chlorite schist and inclusions of quartzite and amphibole (Aleksandrowski, 2005).

The native vegetation in the Karkonosze Mts. has had three major phases of transformation during the recent past (17th to 20th century; Bojko and Kabala, 2017): (1) transformation of

spruce forest and mountain dwarf pines in the upper spruce zone into pasture lands, (2) replacement of beech and beech-fir stands by fast-growing spruce or transformation into arable lands (Malkiewicz *et al.*, 2016), (3) degradation of spruce monocultures during the 70's and 80's of the 20th century due to atmospheric pollution (Waroszewski *et al.*, 2009). Timberline fluctuations modify soil development in high mountain regions (Veit, 1993; Tinner *et al.*, 1996; Carnelli *et al.*, 2004; Favilli *et al.*, 2010). In the Karkonosze Mts., timberline reached an altitude of 1000 m a.s.l. during the period 9200 – 8800 BP (Treml *et al.* 2008). Later (ca. 7400 BP), the timberline shifted to 1320 m a.s.l. (Treml and Migoń, 2015). Treml *et al.* (2008) and Treml and Migoń (2015) argue that the maximum timberline position in the Karkonosze was never higher than 1450 m a.s.l. During Middle Ages and the Little Ice Age, timberline responded to climatic oscillation by lowering its position down to 1145 m a.s.l. in the 19th century (Treml and Migoń, 2015). At present, the upper limit of dense spruce forest on Kowarski Grzbiet is approximately at 1100 m a.s.l. The vegetation of the research area is dominated by *Picea abies* forests with *Vaccinium myrtillus* and grasses *(Poa nemoralis*, *Agrostis capillaries*, *Agrostis canina*, *Poa trivialis* and *Festuca pratensis)* on the forest floor. In the lower part of the slope catena, *Betula pendula* and *Sorbus domestica* appear a common admixture to spruce stands. Tree density drops to about 15 – 25% on the summit plateau. More than 90% of the trees at the plateau and in the uppermost part of the slopes are dead due to the afore-mentioned forest decay.

3.Materials and methods

3.1. Soil sampling and description

Five typical soil profiles were investigated along a toposequence on a N facing slope (Fig. 1) of the Kowarski Grzbiet. The soils were described according to the FAO Guidelines (2006) and the soil reference groups identified using the FAO-WRB system (IUSS Working Group WRB, 2015). Three types of samples were taken. i) More than 30 rock fragments were sampled from the E, Bh/Bhs/Bs and BC horizons for a detailed description of parent rock variability throughout the soil profiles. ii) Approximately 2 kg of bulk soil material was taken from every soil horizon for physicochemical analyses. iii) Additionally, undisturbed samples were collected using stainless steel rings for soil bulk density measurement. When a high skeleton content disabled the use of cylinders, soil bulk density was determined by excavating holes (and weighing the excavated material) that were backfilled with a measurable volume of quartz sand. Prior to measurement, the soil samples were dried, crushed and sieved (2 mm).

3.2. Thin-sections

After the preparation of thin sections from rock samples, the petrographic description of the polished slides was carried out using a Leica DM2500P optical microscope in a transmitted light. The modal composition of the rock samples was estimated by point counting using the JMicroVision v1.2.7 software.

3.2. Soil analyses

The total content of soil organic carbon (SOC) was determined by dry combustion at 550 $^{\circ}$C with a CO_2 spectroscopic detection using a Ströhlein CS-mat 5500 analyzer. Soil pH (in 1M KCl) was potentiometrically measured using a solution ratio of 1:2.5. Exchangeable acidity

was extracted with 1M KCl and titrated potentiometrically, while exchangeable ions (Ca^{2+}, Mg^{2+}, K^{+}, Na^{+}) were extracted with 1 M ammonium acetate at pH=7 (Van Reeuwijk, 2002). The concentration of metals in the leachate was determined using inductively coupled plasma optical emission spectrometry ICP-OES. Poorly crystalline and crystalline oxyhydroxides were estimated after dithionite- and oxalate- extraction, and Fe and Al concentration detection with ICP-OES (Thermo Scientific iCAP 7400). After a pretreatment of the samples with 3% H_2O_2, the particle-size distribution was measured using a sieving (sand fraction) and hydrometer method for the determination of the silt and clay fraction (Van Reeuwijk, 2002). Total element contents (Si, Na, Ca, Ti, Mg, Fe, Mn, Al, P, K, Cl and S) were measured by X-ray fluorescence (XRF, SPECTRO X-LAB 2000, SPECTRO Analytical Instruments, Germany).

3.3. Clay mineralogy

The mineralogy of the clay fraction was determined after removal of organic matter with dilute (3%) and Na-acetate buffered H_2O_2 (pH 5), then by dispersion with Calgon and sedimentation in water. In some horizons, mostly Bh and Bhs, poorly crystallised oxyhydroxides disturbed the XRD pattern and had to be eliminated using an oxalate solution. Oriented specimens on glass slides were analysed using X-ray diffraction (XRD, Bruker AXS D8 Advance) in Cu–Kα radiation, in a range 2 - 15° 2θ, steps 0.02°2θ and 2 s/step. The following sample treatments were performed: Mg-saturation, ethylene glycol solvation (EG), and K-saturation. After an initial XRD scan, the K-saturated samples were heated for 2 h at 335 and 550°C, and rescanned after each heating step. The *d*(060) region was studied on randomly oriented specimens that were step-scanned from 58 to 64°2θ with steps of 0.02°2θ at 10 second intervals. Digitised X-ray data in the range of 2 to 15°2θ were corrected for Lorentz and polarisation factors (Moore and Reynolds, 1997). Peak separation and profile

analysis were carried out by Origin PFM™ using the Pearson VII algorithm after smoothing the diffraction patterns by a Fourier transform function. Background values were calculated by means of a non-linear function (polynomial 2nd order function; Lanson, 1997). To check for the presence of kaolinite and imogolite-type material, the DRIFT (Diffuse Reflection Infrared Fourier Transform; Bruker, Tensor 27) measurements were recorded from 4000 to 250 cm^{-1}. Prior to measurement, the samples were dried in the oven at 80°C for 2 hours. The individual spectra were normalized using OPUS 6 software (Bruker, Germany).

3.4. Meteoric ^{10}Be measurements and erosion rates calculations

The abundance of meteoric ^{10}Be was measured in the fine earth of three soil profiles (K1, K4, K5) (fraction ≤2 mm) as suggested by Egli *et al.* (2010) and Zollinger *et al.* (2017). ^{10}Be was extracted using a modified method (Egli *et al.*, 2010) from Horiuchi *et al.* (1999). The $^{10}Be/^{9}Be$ ratios were measured at the ETH Zurich Tandem Accelerator Mass Spectrometry (AMS) facility (Kubik and Christl, 2009) using ETH AMS standards S2007N ($^{10}Be/Be$ = 28.1 x 10^{-12} nominal) and ICN 01-5-1 ($^{10}Be/^{9}Be$ = 2.709 x 10^{-11} nominal) (Nishiizumi *et al.*, 2007) both associated with a ^{10}Be half-life of 1.387±0.012 My.

Knowing the approximate age of the soils (see above; Engel *et al.*, 2013), soil erosion can be determined by comparing the effective abundance of ^{10}Be measured in the soil with the theoretically necessary abundance for that expected age. According to Zollinger *et al.* (2017) soil erosion can be calculated with:

$$E_{soil} = \frac{1}{\rho f C_{10Be}} \left(\frac{\lambda N}{e^{-\lambda t} - 1} + q \right) \quad (1)$$

where E_{soil} = soil erosion rate (in this equation as cm/y), C_{10Be} (atoms/g) = average ^{10}Be in the top eroding horizons, f = fine earth fraction, ρ□□(g/cm^3) = the bulk density of the top

horizons, N (atoms/cm^2) = ^{10}Be inventory in the profile, q (atoms/cm^2/y) = annual ^{10}Be deposition rate (calculated according to Monaghan *et al.*, 1985/1986; Maejima *et al.*, 2005), λ (4.997 x 10^{-7}/y) = decay constant of ^{10}Be and t (y) = surface age. Average concentrations of ^{10}Be in rainfall are near 1 – 1.5 × 10^4 atoms/cm^3; values that were confirmed also by other investigations (Vonmoos *et al.*, 2006; Heikkilä *et al.*, 2008a,b; Graly *et al.*, 2011)..One problem is that C_{10Be} evolves over time (Zollinger *et al.*, 2017). This can approximately be solved by using an average value of C_{10Be} between t = 0 and t (corresponding to ~ 0.5 × $C_{10Be(today)}$) and by assuming that erosion losses are concentrated on the topsoil horizon (e.g. 0 – 20 cm). For comparison, an additional, often applied procedure (Lal, 2001) to estimate erosion rates using meteoric ^{10}Be was used. The soil erosion (E_{soil}) rate is given by:

$$E_{soil} = z_0 K_E \tag{2}$$

and:

$$K_E = \frac{N_D}{N_S}\left[\frac{Q + q_a}{N_D}\right] - \lambda \tag{3}$$

where z_0 (cm) = thickness of topsoil horizons (comprising O and A horizon), K_E = first order rate constant for removal of soil from the topsoil layer, N_D (atoms/cm^2) = ^{10}Be inventory in the D layer (= remainder of the soil profile comprising B and C horizons, N_S (atoms/cm^2) = ^{10}Be inventory in topsoil horizons, Q (atoms/cm^2/y) = flux of atmospheric ^{10}Be into the topsoil and q_a (atoms/cm^2/y) = flux of meteoric ^{10}Be.

3.5. Pollen analyses

Palynological methods are a useful tool to track signs of past slope processes giving rise to soil layering and induced soil polygenesis (Waroszewski *et al.*, 2015). It is important to note that pollens are stable in a strongly acidic environment (Hicks and Hyvarinen, 1999) and that they can provide valuable data about vegetation shifts in multi-layered materials (Waroszewski *et al.*, 2013). We collected 35 undisturbed soil samples (volume of 1.5 cm^3), starting from the O horizon with 5-10 cm increments (depending on the amount of coarse fragments). The samples were prepared according to Moore et al (1991), which included the following procedure: (1) treatment with HCl, KOH, HF, (2) ACETOLYSIS, (3) MOUNTING IN GLYCEROL AND (4) STAINING WITH FUCHSINE. At least 1000 pollen grains per soil sample were identified and counted using an optical microscope (Axiostar, Zeiss) with a magnification of 400×. For each sample, at least 2 – 4 specimens were prepared. The taxa were divided into 4 groups of species: coniferous trees, deciduous trees and shrubs, perennials and herbaceous plants and cryptogams. The pollen diagram was plotted using POLPAL for Windows (Nalepka and Walanus, 2003). The pollens appeared to be very well preserved and rich in taxa in 27 samples. In the other 8 samples, from the Bs or BC horizons, an insufficient content or no pollens were recorded.

4. Results

4.1. Soil morphology and layering

According to the morphology and particle size distribution along the studied catena, the soils can be assigned to two groups: (1) pedons situated in upper and middle slope positions (K1 – K3) and (2) pedons in the lower-slope (soils K4 – K5). The first three profiles have many similar features. The topsoil is strongly bleached and contains a relatively low amount of

coarse fragments that are often arranged vertically (Table 3). The surface horizons have a distinctly higher silt content (29 – 38%) compared to the subsurface horizons (15 – 25%, Table 4). The fine earth has a friable consistence and an angular structure. The boundary between the topsoil and subsurface layers was clear and wavy. The subsurface horizons (2Bh/2Bhs/2Bs/2BC) have a considerable proportion of rock fragments that are very tightly packed in the lateral position (parallel to slope surface). The texture is coarser directly below the topsoil (loamy sand) and becomes finer with soil depth (sandy loam). Subsoil layers are more compacted (firm consistency) and have a subangular/angular (2Bh/2Bhs) to platy structure (2Bs, 2BC). In profile K1 two continuous stone lines were distinguished; the first one at 20 cm depth, between the E and 2Bh horizon, and the second one (discontinuous) at a depth of 55 cm (Fig. 2).

Profile K4 is formed from a more homogenous material, having a sandy loam texture throughout. Only the topsoil (EB) has a slightly higher silt content (Table 4). Soil structure and rock abundance change at the contact to the 2Bw and 3BC horizon. Three distinct layers can be distinguished: (1) a silty layer hosting an EB horizon with vertically arranged coarse fragments, (2) a 2Bw horizons havig fine subangular/angular aggregates and ca. 30% of coarse fragments and (3) a layer hosting the 3BC and 3C horizon having 70% of coarse fragments and a platy/angular-platy structure. The upper mineral horizons usually have a friable consistence, whereas the subsoil is apparently firm.

Profile K5 consists of two mineral layers: (1) a friable topsoil having a moderate angular structure and a silt loam texture (52 – 56% of silt) and a low content of flat rock fragments that are arranged laterally, and (2) loamy subsoil that still has a high silt proportion (46 – 50%), but many rock fragments, strong platy structure and firm/very firm consistence. Below the depth of 50 cm, the clasts are piled upon each other and the fine earths have a strong platy structure.

4.2. Rock fragments

The rock material (skeleton fraction) sampled from the E and 2Bh horizons of profiles K1, K2 and K3 is a metamorphic garnet mica schist (Fig. 3a, 3b). The rock material contains muscovite (55% vol.) and quartz (28% vol.) as major minerals with a minor contribution of chlorite (7% vol.) and garnet (5% vol.) plus accessory opaque minerals (<5% vol.) and biotite (<1% vol.). It has a medium grained and porphyroblastic texture and exhibits a preferred orientation resulting from the alignment of asymmetric grains. IN CONTRAST, the rock material from the 2Bhs and 3BC horizons of the first three profiles can be classified as amphibole schist (Fig. 3c, 3d). It consists of amphibole (57% vol.) and quartz (35% vol.) as major components, as well as opaque minerals (8% vol.) and accessory garnet, titanite and biotite (all together <1% vol.). This rock has a medium grained texture and has a preferred orientation resulting from the alignment of asymmetric grains of amphibole. The amount of amphibole schists (by volume) decreases in the subsoil layers along the catena in the following order: K1>K2>K3.

Different types of rock material were recognised in the profiles K4 and K5. The rock material of the upper part of the K4 and K5 profiles (Eg/EBg horizons) is a mica schist (Figure 3e, 3f) having muscovite (38% vol.), quartz (36% vol.) and chlorite (14% vol.) as major components and titanite, opaque minerals (all together 9% vol.) and accessory garnet (2% vol.) as minor components. The rock has a medium grained texture and alternately arranged mica-enriched and quartz-enriched layers. No amphibole schist was found. The material sampled in the 2Bw2/3BC horizon of the profile K4 and 2Bwg/3BC of the profile K5 is a gneiss (Fig. 3g,h) that consists of alkali feldspar (38% vol.), quartz (32% vol.) and muscovite (21% vol.) as major components, and chlorite (7% vol.), accessory opaque minerals (3% vol.) and garnet (<1% vol.) as minor components. The rock has a coarse-grained texture and preferred orientation of muscovite and chlorite flakes. Amphibole schist was not identified.

4.3. Physicochemical soil properties

All soils have a very low pH_{KCl} (2.4 – 3.1) in the topsoil (AE, Eg horizon), increasing with depth to 3.0 – 4.1 in Bh or Bhs horizons, and to 3.8 – 4.3 in the BC horizons (Table 5). In contrast to the pH, the exchangeable acidity in general decreased with depth; however, it has the however the highest – in the Bh horizon, apparently in relation to the organic matter distribution (Table 5). The sum of the base cations (BC) is very low and did not exceed 1 cmol(+) kg^{-1} in most horizons. A low BC content is common in soils developed from granite and carbonate-free metamorphic and sedimentary rocks in the Sudeten Mts. (Gałka *et al.*, 2013; Kabala *et al.*, 2013). Base saturation did not exceed 30% and the lowest values were usually measured in the Bh horizon (9 – 12%, Table 5).

The vertical distribution of oxalate- and dithionite-extractable Fe and Al indicates an advanced podzolisation in the first three profiles. The topsoil horizons (AE, E) are strongly depleted in Fe and Al, whereas a significant enrichment is measured in the Bh or Bhs horizon. The values of the podzolisation index (Al_o+1/2Fe_o) are in the Bh horizon of K1 – 3 much higher than in the E horizon (Table 5), which is typical for a strong leaching of Fe and Al (Waroszewski *et al.*, 2015a).

The topsoil horizons of profile K4 have approx. 2% Fe_d and Fe_o, while the subsoil (2Bw2 and 3BC horizons) contains three times less iron (Table 5). In the K5 profile, the vertical distribution of Fe sesquioxides is rather uniform, whereas the Al concentration increases with depth. Also the profiles K4 and K5 have high values of the podzolisation index (Al_o+1/2Fe_o) in the B horizon, but the difference between the B and E/EB horizon is lower compared to K1 – 3.

4.5. Soil geochemistry

All soils are characterised by a high content of silica (47.4 – 75.2%) and aluminium (12.6 – 15.3%) due the prevalence of silicates/aluminosilicates in the parent rock (Table 6). The subsoil of profile K1 has a relatively high content of Fe_2O_3, MgO, CaO and TiO_2, most likely due to the presence of some amphiboles. This is also the case for profile K4 but to a lesser extent (Table 6). The high content of the elements Ba and Hf in the topsoils, particular in profile K1, may be indicative of an aeolian silt addition to soil (Schreib *et al.*, 2014).

4.6. Clay mineralogy

The major components of the clay fraction are mica (peak near 1.0 nm; Mg- and K-saturation and EG-solvation), vermiculite, hydroxy-interlayered vermiculite (peak near 1.4 nm; Mg- and K-saturation and EG-solvation) and mixed-layered phyllosilicates (peak in the range of 1.15 – 1.25 nm). Particularly in the E horizons interstratified phases were recognised after glycol solvation indicated by peaks at 1.22 nm. Some regularly-interstratified phyllosilicates are present to a low amount (recognisable with peaks at 1.7 and 2.5 nm). Traces of smectite can also be detected (as peaks near 1.6 nm) mostly in the topsoil horizons (Fig. 4). The peak at 0.72 nm can be attributed to kaolinite (confirmed with DRIFT measurements) and chlorite (peak around 1.4 nm after heating at 550 °C). Chlorite was present in the subsoil. It strongly decreased towards the surface.

The XRD patterns across the soil catena often showed a peak at 0.85 nm that can be attributed to amphibole (Figs. 4 and 5). It mostly appears in the subsoil (2Bhs or 3BC horizons) of the first two profiles and less pronounced in the 2BC horizon of profile K3. The occurrence of amphibole in the clay fraction in the lowermost horizons is associated to the presence of amphibole schists, while a lack of amphibole in the E horizons relates to either a different lithology (mica schists) or weathering (dissolution and/or transformation of

amphibole). In profile K4 a clear amphibole peak was detected in all soil horizons. This finding is stands in contrast to the absence of amphibolite in the rock fragments. This phenomenon therefore indicates a colluvial contribution in this slope section. If the upper slope is considered as the source area, then the horizons hosting amphibole schists (present in the subsoil Bs, BC and C horizons in the profiles K1-K3) were once exposed to the surface in the past. In profile K5, no amphibole was detected. The extension of the 'amphibolitic' colluvium material ends, therefore, somewhere between K4 and K5.

With the DRIFT measurements, two pronounced peaks at 3694 cm^{-1} and 3620 cm^{-1} were detected that can be attributed to kaolinite (OH-stretching region). The band at 3428 cm^{-1} (chlorite) was found only in the BC horizon of the first two profiles. The weakly developed Si-O stretching band at around 1030 cm^{-1} was attributed to newly-forming dioctahedral phases and the vibration found at circa 1020 cm^{-1} is typical for trioctahedral sheet silicates. These peaks were not recognised in the illuvial horizon of profile K2 and K4 and BC horizon of profile K1. Quartz was identified by the peak doublet at 780 and 800 cm^{-1}. The peaks near 531 and 474 cm^{-1} correspond to illite/muscovite.

4.7. Palynological analyses

In the organic horizon (Oe), the proportion of *Alnus* (alder) and *Corylus* (hazel) and of *Fagus* (beech) *Carpinus* (hornbeam), *Quercus* (oak) and *Tilia* (linden) was lower than in the underlying E horizon, while the share of coniferous species (mainly *Pinus* (pine), *Picea* (spruce)) together with *Betula* (birch) was higher. At the interface of organic and mineral horizons, the sum of NAP increased to 60%. Typical species that are indicative of human activity appear, e.g.: *Sambucus (elder)*, *Galium (cleaver)*, *Plantago lanceolata (ribwort)*, *Lonicera*.

In the E horizons, *Corylus* and *Alnus* reach their maximum with values up to 35% and 26%, respectively. The E horizon has a high percentage of *Quercus*, *Carpinus* and *Fagus* pollen (Fig.7). *Populus* (poplar) pollens (2 – 5%) appear only in the E horizon or at the contact to the O layer. This suggests a disturbance in the woodland structure.

The subsoil B horizon of the first four profiles (K1 – K4) are dominated by *Corylus* (hazel; 15 – 35%), *Alnus* (5 – 23%) and *Pinus* (5 – 30%) pollen. *Quercus*, *Fagus*, *Abies* (fir) are minor constituents of the pollen spectra (Fig. 6). An important component of the illuvial horizon is *Tilia*. Despite the low content (always around 5%) it shows a decreasing trend towards the top. In the 2Bw1 horizon of profile K4, sporomorphs of *Hedera* (ivy) and *Viscum* (mistletoe) were identified. In addition, the presence of *Populus* may speak for a change in the forest density. In profile K4, the presence of *Hedera* and *Humulus* (hop) pollen may also be the result of long distance transport.

Profile K5 showed a different pollen distribution and reflected a strong stratification of the soil material. The topsoil E horizon (1 – 22 cm) was characterised by a high proportion of *Pinus*, *Picea* and *Quercus*, while *Fagus*, *Tilia* and *Carpinus* were absent. Human-induced plants are represented by *Plantago*, Chenopodiaceae (amaranth family) and Roseaceae (rose family). In the EB horizon (at a depth of 22 – 35 cm), *Carpinus* was detected together with a distinct signal from *Plantago, Galium, Thalictrum* (meadow rue)*, Rumex* (dock)*, Cerealia, and Secale* (rye). The appearance of syntrophic species in a single horizon confirms a lithological stratification (Waroszewski *et al.*, 2013). The subsoil horizon 2Bwg (44 – 47 cm) is dominated by *Alnus*, *Betula, Picea, Abies* and *Fagus* sporomorphs. *Ulmus* (elm)*, Tilia, Pinus* and *Quercus* are concomitant species.

4.8. ^{10}Be concentrations and erosion rates

^{10}Be contents in the three soil profiles are given in Table 8. The ^{10}Be-contents ranged from about 0.06 to 3 (x10^{8}) atoms g^{-1}. In all soils, a rather low amount of ^{10}Be was detected in the surface horizons which could be due to (i) leaching of ^{10}Be from these horizons or (ii) erosion or other slope processes (less weathered and/or younger material was added on the top of the soils). The maximum concentration was found in the Bs and BC horizon from where it usually decreased with depth.

Besides the calculation procedure (equation 1 or 3), the erosion rates are the highest for profile K1. The determined rates are between 6.4 and 10.2 t ha^{-1} a^{-1}, depending on the model applied. The other two profiles (K4 and K5) yielded comparable values in the range of 1.3 to 2.9 t ha^{-1} a^{-1}. The profile K4 seems to have the lowest erosion rate (with 1.3 t ha^{-1} a^{-1}). Due to the fact that the uppermost layer of the soils (colluvium) most likely has a different origin, the erosion calculations should be reconsidered. If in profile K1 the subsurface layer instead of the topsoil horizon is used for the calculations, then much lower rates are obtained, (2.0 and 4.1 t ha^{-1} a^{-1}). The erosion rates for profiles K4 and K5 are lower, i.e. 0.7 – 0.8 t ha^{-1} a^{-1} and 1.6 – 2.2 t ha^{-1} a^{-1}, respectively.

5. Discussion

Soil profile stratification was evidenced by soil morphological features, the petrology of the rock fragments, soil texture, soil geochemistry and meteoric ^{10}Be. This stratification is caused by slope processes (erosion, accumulation) and probably also by aeolian silt input.

5.1. Erosion rates

Meteoric ^{10}Be reaches the soil surface, where it can be accumulated, removed laterally due to surface erosion or may infiltrate into the soil (Egli *et al.*, 2010, Maejima *et al.*, 2004, Tsai *et al.*, 2008). The models of erosion intensity typically ignore losses with soil water infiltration and evaluate Be losses due to surface denudation (Lal, 2001). However, an increase of ^{10}Be content in the subsurface Bs or Bhs horizons of the investigated soils was detected, which may either indicate a vertical translocation of ^{10}Be or stratification resulting from the burial of a ^{10}Be-enriched surface layer. The great variability of the ^{10}Be depth profiles can often be explained by complex geochemical and transport mechanisms (Tsai *et al.*, 2008). Eluviation/illuviation-related distribution is crucial for Podzols and Luvisols (Pavich *et al.*, 1984; Tsai *et al.*, 2008). Egli *et al.* (2010) demonstrated a positive correlation between ^{10}Be and Fe_o, Al_o and organic carbon in Podzols and, thus concluded that a downward migration of ^{10}Be together with Fe, Al and/or organic matter takes place. Be therefore may be involved in podzolisation processes.

According to Maejima *et al.* (2004, 2005) and Wyshnytzky *et al.* (2015), meteoric ^{10}Be and clay concentrations, generally decrease with depth and highest concentrations of ^{10}Be in horizons coincide with highest clay concentrations. This suggests that ^{10}Be is adsorbed onto clay surfaces and may take place in clay-mediated transport processes (like in Luvisols). Wyshnytzky *et al.* (2015), however, demonstrated that the relationships of ^{10}Be, clay and secondary Fe-forms (Fe_d) in depth profiles vary considerably between hillslope sites and stable landforms. On low-slope hillslopes and stable landforms, meteoric ^{10}Be, Fe_d, and clay accumulate through time and display clear patterns consistent with soil-horizon development and landform stability.

A clear and positive correlation between ^{10}Be, soil pH and Al_d (Fig. 7) and Al_o (not shown) was found in the investigated soils. To a certain degree, the mobility of ^{10}Be is related to soil

acidity and Al-forms. ^{10}Be reached the highest concentration in the subsurface Bhs, Bw and even BC horizons where the concentration of mobile Al was the highest. This was usually at a greater depth than the maximum accumulation of SOC and mobile Fe forms. It seems that ^{10}Be was to a certain extent translocated within the profiles over podzolisation processes. In contrast to findings of Maejima *et al.* (2004, 2005) but in line with Egli *et al.* (2010), no correlation was found between the clay and ^{10}Be content. This might be related to both, a low clay content in the soils under investigation, the predominance of podzolisation or profile discontinuities. The rather uncommon (negative correlation with org. C) or non-existing correlations (Fe_d or Fe_o) indeed indicate that the investigated soils are probably subjected to downslope movements.

The estimated erosion rates for profile K1 are very high with 6.4 – 10.2 t ha^{-1} a^{-1} (equivalent to 640 – 1020 t km^{-2} a^{-1}). In terms of soil thickness (assuming a soil density of 1.0 to 1.8 kg dm^{-3}), this would correspond to a soil thinning of approx. 360 – 1000 mm ky^{-1} which is considerable for natural, alpine sites (Egli *et al.*, 2010). This would mean that a complete soil profile is removed within less than 1000 years. The other soils (K4 and K5) exhibit an erosion rate in the range of approx. 50 – 290 mm ky^{-1}. When modelling erosion rates using meteoric ^{10}Be then the precipitation rates over time should be known. This is, however, often not the really the case. Unfortunately, (modelling) data about annual precipitation rates over the entire Holocene are not available for our investigation area. We therefore had to assume that the average present-day (i.e. for the last about 100 years) precipitation rates represent the situation for the Holocene. In a first attempt, this approach is certainly not wrong. The Holocene began about 11500 years ago and corresponds to the present interglacial. Compared to the previous and older glacial stages, this period is characterised by a highly stable climate (Desmet *et al.*, 2005).

If the uppermost layer (colluvium), that seems to have a different origin, is ignored in the erosion calculations, then lower rates are obtained (second scenario; Table 7). For K1, 200 – 410 t km^{-2} a^{-1} are calculated corresponding to 110 – 410 mm ky^{-1}. The sites K4 and K5 would exhibit under such condition erosion rates in the range of 40 – 120 mm ky^{-1} (70 – 220 t km^{-2} a^{-1}). These values (second scenario) better lie in the range that is commonly measured in alpine and mountainous regions. Riebe *et al.* (2004) report values in the range of 87 – 132 t km^{-2} yr^{-1}. According to a data compilation of Dixon and von Blanckenburg (2012), erosion rates may vary between <1 and 300 t km^{-2} yr^{-1} before they are decoupled from chemical weathering. An even larger range was measured in the New Zealand Alps with values from about 4 to about 2000 t km^{-2} yr^{-1}. This comparison again shows that the erosion measured at site K1 is rather at the upper end where soil formation and weathering still can cope with erosion. The other two sites (K4 and K5), however, represent typical erosion values on hill slopes. Based on the calculations of the second scenario, the erosion rates are much lower for K1 and, thus, the values would lie in a middle range of the observations. We therefore have to assume, that the second scenario better represents reality.

These considerations however show the difficulties in the used methodology. Due to the complex structure of the soil, the applicability of meteoric ^{10}Be as a tracer for soil erosion is not that straightforward anymore.

5.2. Aeolian input into soils

The geochemical and mineralogical data suggest that soil formation and properties are controlled by both, local bedrock and aeolian input. The partially abrupt changes in the silt fraction from one horizon to another seem to be due to aeolian influence. It seems unlikely that the short-distance water erosion may result in a selective silt accumulation to such an extent (Malkiewicz *et al.*, 2016; Migoń and Kacprzak, 2014). An aeolian input into the soils

of the Karkonosze Mts. was not verified so far, but several indirect indications support such a possibility, including (i) the occurrence of loess covers on the northern foothills and lower slopes of the Sudeten mountains, (ii) the presence of loess covers in isolated, intra-mountain basins such as the Klodzko Basin (see below), (iii) and enrichment of silt in soils of all ranges of the Sudeten mountains, irrespective of the bedrock type (Kabala *et al.*, 2015).

Moreover, the relatively high elemental contents of Hf in the topsoil of K1 are indicative of aeolian input, as mentioned by many authors (Liator, 1987; Dahms, 1993; Küfmann, 2003; Muhs and Benedict, 2006; Munroe *et al.*, 2007; Lin and Feng, 2013; Geitner *et al.*, 2014; Scheib *et al.*, 2014; Waroszewski *et al.*, n.d.). Also, the Zr and Ba contents are much higher in the topsoil than in subsoil horizons and point to a potential aeolian input. An aeolian contribution to soils is a doubtless phenomenon in many mountain areas (Boulding and Boulding, 1981; Küfmann, 2008; Mason *et al.*, 2011; Geitner *et al.*, 2014; Gild *et al.*, 2018; Waroszewski *et al.*, n.d.). A major aeolian silt contributions to soils in the Karkonosze Mts. seems to have happened in the late Pleistocene (Pleniglacial), when large-scale eolian accumulation took place in the Sudeten foothills (Badura and Jary, 2012). Recent OSL dating of shallow loess covers in the Sudeten foothills and the intra-mountain Klodzko Basin indicate an age of 16 – 20 ka years (Waroszewski *et al.*, unpublished data). During this period, the Karkonosze Mts were locally covered with small glaciers (Engel *et al.*, 2014; Traczyk i Migoń, 2000), but all other areas could have received the aeolian input.

5.3. A model of landscape and soil evolution

The relatively well-preserved topsoil layers — having more aeolian silt and a higher Hf content — may indicate a rather old (late Pleistocene) age and, thus, stability of the stratified cover bed. However, the presence of *Fagus sylvatica* and *Abies* pollen in the subsurface B horizon support a much younger age (late Holocene), because these species appeared at the

earliest in the Karkonosze Mts in the late Atlantic/early Sub-Boreal period (Malkiewicz *et al.*, 2016). It seems unlikely that these pollens migrated along the soil profile. Podzols of the upper forest zone in the Sudeten Mts typically have the humus form mor that is considered to be almost inactive in terms of faunal activity and therefore bioturbation (Bojko and Kabala, 2017; Labaz *et al.*, 2014). It seems more likely that tree pollens are more or less stable in a specific layer. This consequently leads to the subsequent landscape and soil evolution scenario:

Cambisol-like soils persisted under mixed-species forests until about the Sub-Boreal or even Sub-Atlantic period. Only relatively 'recently', these soils were covered by a silt-enriched thin surface layer (due to erosion and deposition; Fig. 8). This scenario assumes a long-term preservation of silt-enriched zones (from aeolian accumulation) at least in some parts of the flattened summit area under native vegetation. With this scenario, the soils of the upper zone are polygenetic. They are hypothesised to have had the following development sequence: cryogenic soils in the late Pleistocene, Dystric Cambisols during the early Holocene period, and Podzols in the late Holocene period. At the end of the Pleistocene and in the beginning of the Holocene, Cryosols existed in the upper and mid slope sections that developed from amphibole schists (K1, K2, K3) and from mica/gneiss in the lower slope section (profile K5). This development corresponds with the present-day Bs, BC and C horizons that were exposed in the past to the surface. The cold climate and cryoturbation processes at this time are evidenced by the following features: involute stone line in profile K1, platy soil structure, rock arrangement especially in K1 and K5 (Table 3) and a lack of pollen (no vegetation/ elimination of spores by physical and chemical weathering) in all previously mentioned soils. Part of the amphibole schists strata situated at the top parts of the ridge were subsequently eroded (in K1 profile, we calculated high erosion rates) and deposited in the lower part of mid slope section (e.g. also evidenced by the presence of amphibole in the clay fraction of

profile K4; Fig. 8). The results obtained from pollen analysis (dominance of *Ulmus-Corylus* with traces of *Humulus* and *Hedera helix*) from profile K4 suggest that erosion started during the late Boreal (if we considered long distance transport of *Humulus* and *Hedera helix* pollens) or at the beginning of the Atlantic. This is confirmed by several other investigations in the Alps where an increased erosion rate during this period was detected – although this increase was not everywhere due to climate changes but also due to a starting human impact (Bajard *et al.*, 2016; Boxleitner *et al.*, 2017). The increasing erosion Karkonosze mountains correlates with the rapid climate shift evidenced by thick sand deposits in the Wielki Staw Lake (Malkiewicz *et al.*, 2016) having an age of 8359 – 8539 cal BP or other sand strata documented in peat of the Izerskie Mts. formed at a similar period (Baranowska-Kącka, 2003). The top 10 cm of profile K4 represent a younger pollen archive (Fig. 6) that may be related to a second phase of deposition during the Sub-Atlantic.

During the 'Atlantic optimum', the slopes were stabilised (Chmal and Traczyk, 1993) and a progressive phase of soil development has taken place (Malkiewicz *et al.*, 2016). A new pulse of slope activity is characterised by aeolian deposition at the plateau and upper slope zones. The low age of the superimposed silt material is confirmed with low ^{10}Be concentrations and the pollen assemblage (high share of *Carpinus, Corylus, Quercus* and *Fagus*) that indicated a Sub-Boreal period (Malkiewicz *et al.*, 2016). Along the slope, the aeolian silt was partially eroded and mixed into the soils situated at mid and to lower slope positions. After the expansion of *Picea abies* forests, the soils having silt strata started to transform into Podzols (Waroszewski *et al.*, 2013).

The subsoil (BC and C horizons) of profile K5 has typical Pleistocene features, the top soil material, however, seems younger. The material that nowadays exhibits the Esg, EBg and Bsg horizons, was deposited over a solifluction stratum probably at the turn of the Sub-Boreal to the Sub-Atlantic period. Down to the depth of about 50 cm pollens of *Fagus* and

Abies were found which are typical for a later Holocene age, which argues for their young age (late Holocene). In addition, the presence of *Carpinus, Cerealia, Chenopodiacea, Humulus, Viscum, Thalictrum* and *Plantago* indicate human-induced changes (Dudová *et al.*, 2012; Jäger *et al.*, 2015; Mendyk *et al.*, 2016; Glina *et al.*, 2016) that are typical for the late Sub-Atlantic. Despite the high content of silt in the topsoil, the upper or medium slope positions that are rich in amphibole schists cannot be considered as the source of the colluvial material because of their different lithology (Fig. 3). We therefore assume that this colluvium was transported from neighbouring area were mostly gneisses and mica schists dominate as parent material (Waroszewski *et al.*, 2010). Due to concave slope topography and enhanced soil moisture (Tables 2), podzolisation was less intense, whereas stagnic properties became more dominant features.

6. Conclusions

The applied multidisciplinary approach (palynological, mineralogical and soil chemical analyses, analysis of cosmogenic nuclides) confirmed our hypothesis and clearly demonstrated that soil and landscape evolution in the Karkonosze Mountains has been complex. The different strata detected in the soils have either an aeolian origin or are related to mass wasting. Together with the pollen assemblage, timings for the progressive and regressive soil forming phases could be proposed.

According to our results, some aeolian input to soils (Crysols) and slope sediments must have occurred in the late Pleistocene. Physico-chemical and mineralogical analyses indicated that the material was denudated from the ridge and upper slope positions (regressive phase) forming a colluvium at midslope positions. With the help of pollen analyses, the timing of this processes could be fixed to the transition of the late Boreal to the Atlantic (Holocene). Later, during the Sub-Boreal, a mass wasting of some remains of the silt material deposited at

the end of the Pleistocene age on the ridge top seems to have occurred. In combination with the vegetation whose litter gave rise to a further soil acidification, the Leptosols/Cambisols transformed into Podzols at upper slope or shoulder positions and to Albic Cambisols at midslope positions (progressive phases). At the lower part of the slope catena, also Stagnosols started to form.

Using ^{10}Be as a tracer, relatively high erosion rates at the top of the investigated catena were confirmed. The mid/lowermost part of the catena exhibited lower erosion rates. The Bs, BC, C horizons were exposed over a relatively long period. The low ^{10}Be content in the uppermost soil layer (here a colluvium) supports the hypothesis of erosion and deposition, but also the effect podzolisation may have given its contribution. However, the determination of erosion rates remains under such complex conditions is difficult. Together with the results from clay mineralogy, the extent of the deposited, amphibole-rich material could be traced. Slope processes and soil formation are very complex. Using a multi-method approach, this complexity can at least partially be traced.

Acknowledgements

This research was partially financed by NCN (project nr 2014/15/D/ST10/04087) and Sciex NMCx (nr 12.624). We would like to express our appreciation to Maria Budzisz - Waroszewska, Małgorzata Chilkiewicz , Janusz Kamiński , Dorota Ciszek and Robert Nawrocki for their assistance during field campaigns. We are indebted to two anonymous reviewers and Editor Fiona Kirkby for their constructive remarks and comments on an earlier version of the manuscript.

References

Aleksandrowski, P., Słaby, E., Szuszkiewicz, A., Galbarczyk-Gąsiorowska, L., Madej, S., Szełęg, E., 2014. Geological structure. In: Knapik, R., Raj, A. (Eds.), Nature of Karkonosze Mts. National Park. Karkonoski Park Narodowy, Jelenia Góra, pp. 7–46 (in Polish).

Allen C.E., Darmody R.G., Thorn C.E., Dixon J.C., Schlyter P., 2001. Clay mineralogy, chemical weathering and landsape evolution in Arctic-Alpine Sweden. Geoderma 99, 277-294.

Bajard, M., Sabatier, P., David, F., Develle, A.-L., Reyss, J.-L., Fanget, B., Malet, E., Arnaud, D., Augustin, L., Crouzet, C., Poulenard, J., Arnaud, F., 2016. Erosion record in Lake La Thuile sediments (Prealps, France): Evidence of montane landscape dynamics throughout the Holocene. The Holocene 26, 350-364.

Baruck J., Nestroy O., Sartori G., Baize D., Traidl R ., Vrščaj B ., Bräm E ., Gruber F.E., Heinrich K., Geitner C., 2016. Soil classification and mapping in the Alps: The current state and future challenges. Geoderma 264, 312-331.

Birkeland P.W., Shroba R.R., Burns S.F., Price A.B., Tonkin P.J., 2003. Integrating soils and geomorphology in mountains – an example from the Front Range of Colorado. Geomorphology 55, 329-344.

Bojko O., Kabala C. 2016. Transformation of physicochemical soil properties along a mountain slope due to land management and climate changes – a case study from the Karkonosze Mountains, SW Poland. Catena 140, 43-54.

Bojko, O., Kabala, C. 2017. Organic carbon pools in mountain soils — Sources of variability and predicted changes in relation to climate and land use changes. Catena 149, 209-220.

Boulding, B. H., Boulding, J. R., 1981. Genesis of silty and clayey material in some alpine soils in Teton Mountains, Wyoming and Idaho. Indiana Academy of Science Proceedings 91, 552–562.

Boxleitner, M., Musso, A., Waroszewski, J., Malkiewicz, M., Maisch, M., Dahms, D., Brandová, D., Christl, M., de Castro Portes, R., Egli, M., 2017. Late Pleistocene – Holocene surface processes and landscape evolution in the central Swiss Alps. Geomorphology 295, 306-322.

Brisset, E., Miramont. C., Guiter, F., Anthony, E., Tachikawa, K., Poulenard, J., Arnaud, F., Delhon, C., Meunier, J.-D., Bard, E., Sumera, F., 2013. Non- reversible geosystem destabilisation at 4200 cal. BP: sedimentological, geochemical and botanical markers of soil erosion recorded in a Mediterranean Alpine Lake. The Holocene 23, 1863–1874.

Butler, B.E., 1959. Periodic phenomena in landscapes as a basis for soil studies. Aust. CSIRO Soil Publ. 14, 1–10.

Carnelli, A.L., Theurillat, J-P., Thinon, M., Vadi, G., Talon, B., 2004. Past uppermost tree limit in the Central European Alps (Switzerland) based on soil and soil charcoal. The Holocene 14, 393–405.

Chmal, H., Traczyk, A., 1993. Plejstoceńskie lodowce gruzowe w Karkonoszach . Czas. Geogr. 64 (3–4), 253–262.

Chmal H., Traczyk A., 1998. Postglacial development of the Karkonosze Mountains and Izerskie Mountains relief in the basis of the analysis of fluvial, lacustrine and slope sediments. In: Sarosiek J. and Štursa J., (eds) Geoecological Problems of the Karkonosze Mountains. Poznan: Acarus, pp. 81–87 (in Polish).

Coutard, J.-P., and Francou, B., 1989: Rock temperature measurements in two alpine environments: implications for frost weathering. Arctic and Alpine Research, 21, 399–416.

Dahms D.E., 1993. Mineralogical evidence of eolian contribution to soils of late Quaternary moraines, Wind River range, Wyoming, USA. Geoderma 59, 175-196.

Desmet, M., Mélières, M.-A., Arnaud, F., Chapron, E., Lotter, A.F., 2005. Holocene climates in the Alps: towards a common framework – an introduction. Boreas 34, 401-403.

Dixon JL, von Blanckenburg F. 2012. Soils as pacemakers and limiters of global silicate weathering. Comptes Rendus Geosciences 344, 596–609.

Dudová L., Hájková P., Buchtova H., Opravilová V., 2012. Formation, succession and landscape history of Central-European summit raised bogs: A multiproxy study from the Hruby Jesenik Mountains. Holocene 23, 230–242.

Egli, M., Mirabella, A., Sartori, G., Fritze P., 2003. Weathering rates as a function of climate: results from a climosequence of the Val Genova (Trentino, Italian Alps). Geoderma 111, 99-121.

Egli, M., Mirabella, A., Mancabelli, A., Sartori, G., 2004. Weathering of soils in alpine areas as influenced by climate and parent material. Clays and Clay Minerals 52, 287-303.

Egli, M., Mirabella, A., Sartori, G. 2008. The role of climate and vegetation in weathering and clay mineral formation in late Quaternary soils of the Swiss and Italian Alps. Geomorphology 102, 307-324.

Egli, M., Brandová, D., Böhlert, R. Favilli, F., Kubik, P., 2010. ^{10}Be inventories in Alpine soils and their potential for dating land surfaces. Geomorphology 119, 62-73.

Engel, Z., Nývlt, D., Křížek, M., Treml, V., Jankovská, V., Lisá, L., 2010. Sedimentary evidence of landscape and climate history since the end of MIS 3 in the Krkonoše Mountains, Czech Republic. Quat. Sci. Rev. 29, 913–927.

Engel, Z., Braucher, R., Traczyk, A., Laetitia, L., ASTER team, 2014. ^{10}Be exposure age chro- nology of the last glaciation in the Krkonoše Mountains, Central Europe. Geomorphology 206, 107–121.

Eze P.N., Meadows M.E., 2014. Texture contrast profile with stonelayer in the Cape Paninsula South Africa: Autochthony and polygenesis. Catena 118, 103-114.

FAO, 2006. Guidelines for Soil Description. 4th ed. FAO, Rome.

Favilli, F., Cherubini, P., Collenberg, M., Egli, M., Sartori, G., Schoch W., Haeberli, W., 2010. Charcoal fragments of Alpine soils as an indicator of landscape evolution during the Holocene in Val di Sole (Trentino, Italy). Holocene 20, 67-79.

Galka, B., Podlaska, M., Kabala, C. 2013. Forest habitats on dystric Cambisols developed from granite in the Stolowe Mountains. Sylwan 157, 385-394.

Geitner, C., Schäfer, D., Bertola, S., Bussemer, S., Heinrich, K., Waroszewski J., 2014. Landscape archaeological results and discussion of Mesolithic research in the Fotsch valley (Tyrol). – In: Kerschner, H., Krainer, K., Spötl C. (Ed.), From the foreland to the Central Alps – Field trips to selected sites of Quaternary research in the Tyrolean and Bavarian Alps (DEUQUA EXCURSIONS), Berlin, pp. 106-115.

Gerrard, A.J., 1981. Soils and Landforms: An Integration of Geomorphology and Pedology. George Allen and Unwin, Boston, MA.

Glina, B., Malkiewicz, M., Mendyk, Ł., Bogacz, A., Woźniczka, P., 2017. Human-affected disturbances in vegetation cover and peatland development in the late Holocene recorded in shallow mountain peatlands (Central Sudetes, SW Poland). Boreas 46(2):294-307.

Gild, C., Geitner, C., Sanders D., 2018. Discovery of a landscape-wide drape of late-glacial aeolian silt in the western Northern Calcareous Alps (Austria): First results and implications. Geomorphology 301, 39-52.

Hicks, S., Hyvarinen, H., 1999. Pollen influx values measured in different sedimentary environments and their palaeoecological implications. Grana 38, 228–242.

Horiuchi, K., Minoura, K., Kobayashi, K., Nakamura, T., Hatori, S., Matsuzaki, H., Kawai, T., 1999. Last-glacial to post-glacial ^{10}Be fluctuations in a sediment core from the Academician Ridge, Lake Baikal. Geophysical Research Letters 26, 1047–1050.

Huggett, R.J., 1975. Soil landscape systems: a model of soil genesis. Geoderma 13, 1–22.

IUSS Working Group WRB, 2015. World Reference Base for Soil Resources 2014, update 2015: International soil classification system for naming soils and creating legends for soil maps. World Soil Resources Reports 106, FAO, Rome.

Jäger H., Achermann M., Waroszewski J., Kabała C., Malkiewicz M., Gärtner H., Dahms D., Krebs R., Egli M., 2015. Pre-alpine mire sediments as a mirror of erosion, soil formation and landscape evolution during the last 45 ka. Catena 128, 63-79.

JOHNSON, D., L. 1990. BIOMANTLE EVOLUTION AND THE REDISTRIBUTION OF EARTH MATERIALS AND ARTIFACTS. SOIL SCIENCE, 149, 84-102.

Johnson, D.L., 1993. Dynamic denudation evolution of tropical, subtropical and temperate landscapes with three-tiered soils: toward a general theory of landscape evolution. Quat. Int. 17, 67–78.

Johnson, D.L., Watson-Stegner, D., 1987. Evolution model of pedogenesis. Soil Science 143, 349–366.

KABAŁA C. (ED.), BEKIER J., BIŃCZYCKI T., BOGACZ A., BOJKO O., CUSKE M., ŚWIELĄG-PIASECKA I., DĘBICKA M., GAŁKA B., GERSZTYN L., GLINA B., JAMROZ E., JEZIERSKI P., KARCZEWSKA A., KASZUBKIEWICZ J., KAWAŁKO D., KIERCZAK J., KOCOWICZ A., KRUPSKI M., KUSZA G., ŁABAZ B., MARZEC M., MEDYŃSKA-JURASZEK A., MUSZTYFAGA E., PERLAK Z., PĘDZIWIATR A., PORA E., PRZYBYŁ A., STRĄCZYŃSKA S., SZOPKA K., TYSZKA R., WAROSZEWSKI J., WEBER J., WOŹNICZKA P. 2015. SOILS OF LOWER SILESIA: ORIGINS, DIVERSITY AND PROTECTION. PTG. PTSH. WROCŁAW, 256 PP.

Kabala, C., Bogacz, A., Łabaz, B., Szopka, K., Waroszewski, J., 2013. Diversity, dynamics and threats of soils. In: Knapik, R., Raj, A. (Eds.), Nature of the Karkonosze National Park. Jelenia Góra, pp. 91–126 (in Polish).

Kabala, C., Bogacz, A., Galka, B., Jezierski, P., Labaz, B., Waroszewski, J., 2013. Cation exchange capacity of soils developed on various bedrock in the Stolowe Mountains. Prace Geograficzne 135, 7-20.

Kasprzak M., Traczyk A., Migała K., Rakowski K., 2016. Does relict permafrost occur in the Karkonosze Mts? 9th Conference Geoecological Problems of the Krkonoše/Karkonosze Mountains 'Past, present and future of transboundary cooperation in research and management. Book of Abstracts, 64-65.

Kleber, A., Terhorst, B., 2013. Mid-latitude slope deposits (Cover Beds). Developments in Sedimentology 66, Elsevier, (302 pp).

Küfmann C., 2003. Soil types and eolian dust in hight mountainous karst of the Northern Calcareous Alps (Zugspitzplatt, Wetterstein Mountains, Germany). Catena 53, 211-227.

Labaz B., Galka B., Bogacz A., Waroszewski J., Kabala C. 2014. Factors influencing humus forms and forest litter properties in the mid-mountains under temperate climate of southwestern Poland. Geoderma 230–231, 265-273.

Lal D. 2001. New nuclear methods for studies of soil dynamics utilizing cosmic ray produced for radionuclides, In *Sustaining the Global Farm*. Stott DE, Mohtar RH, Steinhardt GC. (Eds.). 10th International Soil Conservation Organization Meeting, Purdue University and USDA-ARS National Soil Erosion Research Laboratory, 1044–1052.

Larsen, J.L., Almond, P.C., Eger, A., Stone, J.O., Montgomery, D.R., Malcolm, B., 2014. Rapid soil production and weathering in the Southern Alps, New Zealand. Science 343, 637–640.

Lee S.S., Nagy K.L, Fenter P. 2007. Distribution of barium and fulvic acid at the mica-

solution interface using in-situ X-ray reflectivity. Geochim. Cosmochim. Acta 71, 5763–5781.

Liator M.I., 1987. The influence of eolian dust on the genesis of alpine soils in the front range, Colorado. Soil Science Society of America journal 51, 142-147.

Lin Y.C., Feng J.L., 2013. Aeolian dust contribution to the formation of alpine soils at Amdo (Northern Tibetian plateau). Geoderma 259-260, 104-115.

Lorz, C., 2011. Stratification of the regolith continuum — a key property for processes and functions of landscapes. Z. Geomorphol. 55 (Suppl. 3), 277–292.

Mäilander, R., Veit, H., 2001. Periglacial cover-beds on the Swiss Plateau: indicators of soils, climate and landscape evolution during the Late Quaternary. Catena 45, 251-272.

Maejima, Y., Matsuzaki, H., Nakano, C., 2004. ^{10}Be concentrations of red soils in Southwest Japan and its possibility of dating. Nuclear Instruments and Methods in Physics Research B 223-224, 596-600.

Maejima, Y., Matsuzaki, H., Higashi, T., 2005. Application of cosmogenic ^{10}Be to dating soils on the raised coral reef terraces of Kikai Island, southwest Japan. Geoderma 126, 389-399.

Malkiewicz M., Waroszewski J., Bojko O., Egli M., Kabala C., 2016. Holocene vegetation history and soil development reflected in the lake sediments of the Karkonosze Mountains (Poland). The Holocene 26(6), 890-905.

Mason, J.A., Nater, E.A., Zanner, C.W., Bell, J.C., 1999. A new model of topographic effects on the distribution of loess. Geomorphology 28, 223–236.

Matsuoka, N., 1990: The rate of bedrock weathering by frost action: field measurements and a predictive model. Earth Surface Processes and Landforms 15, 73–90.

MENDYK Ł., MARKIEWICZ M., BEDNAREK R., ŚWITONIAK M., GAMRAT W.W., KRZEŚLAK I., SYKUŁA M., GERSZTYN L., KUPNIEWSKA A., 2016. ENVIRONMENTAL

CHANGES OF A SHALLOW KETTLE LAKE CATCHMENT IN A YOUNG GLACIAL LANDSCAPE (SUMOWSKIE LAKE CATCHMENT), NORTH-CENTRAL POLAND. QUATERNARY INTERNATIONAL 418, 116-131.

Migoń, P., Kacprzak, A., 2014. Lateral diversity of regolith and soils under a mountain slope — implications for interpretation of hillslope materials and processes, central Sudetes, SW Poland. Geomorphology 221, 69–82.

Moore, P.D., Webb, J.A., Collinson, M.E., 1991. Pollen Analysis. Blackwell Scientific Publications, Oxford.

Moore, D.M., Reynolds, R.C., 1997. X-ray Diffraction and the Identification and Analysis of Clay Minerals. 2nd ed. Oxford Univ. Press, New York.

Muhs D.R., Benedict J.B., 2006. Eolian additions to late quaternary alpine soils, Indian Peaks Wilderness Area, Colorado Front range. Arctic, Antarctic and Alpine research 38 (1), 120-130.

Muhs D.R., 2013. The geologic record of dust in Quaternary. Aeolian Research 9, 3-48.

Munroe J.S., Farrugia G., Ryan P.C., 2007. Parent material and chemical weathering in alpine soils on Mt. Mansfield, Vermont, USA. Catena 70, 39-48.

Nalepka D., Walanus A. 2003. Data processing in pollen analysis. ACTA PALAEOBOTANICA 43, 125-134.

Pawlik, L., Migoń, P., Owczarek, P., Kacprzak, A., 2013. Surface processes and interactions with forest vegetation on a steep mudstone slope, Stołowe Mountains, SW Poland. Catena 109, 203–216.

Pavich, M.J., Brown, L., Klein, J., Middleton, R., 1984. ^{10}Be accumulation in a soil chronosequence. Earth and Planetary Science Letters 68, 198-204.

Phillips J.D., 1993. Stability implications of the state factor model of soils as a nonlinear dynamical system. Geoderma 58, 1–15.

Phillips, J.D., 2004. Geogenesis, pedogenesis, and multiple causality in the formation of texture-contrast soils. Catena 58, 275–295.

Phillips, J.D., Lorz, C., 2008. Origins and implications of soils layering. Earth Sci. Rev. 89, 144–155.

Phillips J.D., Šamonil P., Pawlik Ł., Trochta J., Daněk J., 2017. Domination of hillslope denudation by tree uprooting in an old-growth forest. Geomorphology 276, 27-36.

Proust, D., Caillaud, J., Fontaine, C., 2006. Clay minerals in early amphibole weathering: tri- to dioctahedral sequence as a function of crystallization sites in the amphibole. Clays Clay Miner. 54, 351–362.

Riebe, C.S., Kirchner, J.W., Finkel, R.C., 2004. Sharp decrease in long-term chemical weathering rates along an altitudinal transect. Earth and Planetary Science Letters 218, 421-434.

Schaetzl, R.J., 1998. Lithologic discontinuities in some soils on drumlins: theory, detection and application. Soil Sci. 163, 570–590.

Schaetzl, R.J., Loope, W.L., 2008. Evidence for an eolian origin for the silt-enriched soil mantles on the glaciated uplands of eastern Upper Michigan, USA. Geomorphology 100, 285–295.

Scheib, A. J., Birke, M., Dinelli, E., GEMAS Project Team. 2014. Geochemical evidence of aeolian deposits in European soils. Boreas, 43,175–192.

Schmidt, R., Koinig, K.A., Thompson, R., Kamenik, C., 2002. A multi proxy core study of the last 7000 years of climate and alpine land-use impacts on an Austrian mountain lake (Unterer Landschitzsee, Niedere Tauern). Palaeogeography, Palaeoclimatology, Palaeoecology 187(1-2), 101-120.

Simonson, R.W., 1978. A multiple-process model of soil genesis. In: Mahaney, W.C. (Ed.), Quatenary Soils. GeoAbstracts, Norwich, pp. 1–25.

Sobik, M., Błaś, M., Migała, K., Godek, M., Nasiółkowski, T., 2013. Climate. In: Knapik, R., Raj, A. (Eds.), Nature of Karkonosze Mts. National Park. Karkonoski Park Narodowy, Jelenia Góra, pp. 147–187 (in Polish).

Sommer, M., Gerke, H.H., Deumlich, D., 2008. Modelling soil landscape genesis – A "time split" approach for hummocky agricultural landscapes. Geoderma 145, 480-493.

Stückrad, S., Sabel, K.-J., Wilcke, W. 2010. Contributions of different parent materials in soils developed from periglacial cover beds. European Journal of Soil Science 61, 844–853.

Tinner, W., Ammann, B., Germann, P., 1996. Treeline Fluctuations Recorded for 12,500 Years by Soil Profiles, Pollen, and Plant Macrofossils in the Central Swiss Alps. Arctic and Alpine Research, 28(2), 131-147.

Traczyk A., Migon P. 2000. Cold-climate landform patterns in the Sudetes. Effects of lithology, relief and glacial history. Acta Universitatis Carolinae 35, 185-210.

Treml V., Jankovská V., Petr L., 2008. Holocene dynamics of the alpine timberline in the High Su- detes. Biologia 63, 73-80.

Treml, V., Migoń, P. 2015. Controlling factors limiting timber- line position and shifts in the Sudetes – a review. Geographia Polonica 88, 1–16.

Tsai, H., Maejima, Y., Hseu, Z.-Y., 2008. Meteoric ^{10}Be dating of highly weathered soils from fluvial terraces in Taiwan. Quaternary International 188, 185-196.

Újvári, G., Varga, A., Balogh-Brunstad, Z., 2008. Origin, weathering and geochemical composition of loess in southwestern Hungary. Quaternary Research 69, 421–437.

Van Reeuwijk, L.P., 2002. Procedures for Soil Analysis. 6th ed. ISRIC, Wageningen, Netherlands.

Veit, H. 1993. Holocene solifluction in the Austrian and southern Tyrolean Alps: dating and climatic implications. *In:* Frenzel B, editor. Solifluction and Climatic Variation in the

Holocene. ESF Project European Palaeoclimate and Man 6, Paläoklimaforschung 11. Stuttgart: Fischer, 23–32.

Waroszewski J., Kabala C., Szopka K., 2009.Trace elements in soils of upper zone of spruce forest on Szrenica Mount and the Kowarski Grzbiet Range in the Karkonosze Mountains. Journal of Elementology 14(4): 805–814.

Waroszewski, J., Kabała, C., Turska, A. 2010. Specific properties of soils on the Kowarski Grzbiet Ridge in the Karkonosze Mts. Opera Corcontica 47/2010 Suppl. 1, pp. 47-56. (in Polish with English abstract)

Waroszewski, J., Kalinski, K., Malkiewicz, M., Mazurek, R., Kozlowski, G., Kabala, C., 2013. Pleistocene–Holocene cover-beds on granite regolith as parent material for Podzols — an example from the Sudeten mountains. Catena 104, 161–173.

Waroszewski, J., Malkiewicz, M., Mazurek, R., Labaz, B., Jezierski, P., Kabala, C., 2015a. Lithological discontinuities in Podzols developed from sandstone cover beds in the Stolowe Mountains (Poland). Catena 126, 11–19.

Waroszewski, J., Kabala, C., Jezierski, P., 2015b. Relief-induced soil differentiation at the sandstone-mudstone contact in the Stołowe Mountains, SW Poland. Z. Geomorphol. 59 (Suppl. 1), 211–226.

Waroszewski J., Egli M., Kabala C., Kierczak J., Brandova D., 2016. Mass fluxes and clay mineral formation in soils developed on slope deposits of the Kowarski Grzbiet (Karkonosze Mountains, Czech Republic/Poland). Geoderma 264B, 363-378.

Waroszewski, J., Sprafke, T., Kabala, C., Musztyfaga, E., Łabaz, B., Woźniczka, P. (n.d.). Aeolian silt contribution to soils on mountain slopes (Mt. Ślęża, southwest Poland). Quaternary Research, 1-16. doi:10.1017/qua.2017.76

Wyshnytzky, C., Ouimet, W.B., McCarthy, J., Dethier, D.P., Shroba, R.R., Bierman, P.R., Rood, D.H., 2015. Meteoric 10Be, clay, and extractable iron depth profiles in the

Colorado Front Range: Implications for understanding soil mixing and erosion. Catena 127, 32-45.

Yaalon, D.H., Ganor, E., 1973. The influence of dust on soils during the Quaternary. Soil Sci. 116, 146–155.

Zollinger, B.; Alewell, C.; Kneisel, Christof; Meusburger, K.; Brandová, D.; Kubik, P.; Schaller, M.; Ketterer, M.; Egli, M., 2015. The effect of permafrost on time-split soil erosion using radionuclides (^{137}Cs, $^{239+240}$Pu, meteoric ^{10}Be) and stable isotopes (δ^{13}C) in the eastern Swiss Alps. Journal of Soils and Sediments, 15, 1400-1419.

Zollinger, B.; Alewell, C.; Kneisel, C.; Brandová, D.; Petrillo, M.; Plötze, M.; Christl, M.; Egli, M., 2017. Soil formation and weathering in a permafrost environment of the Swiss Alps: a multi-parameter and non-steady-state approach. Earth Surface Processes and Landforms 42, 814-835.

Table 1. Geochronological data related to landscape evolution in the north-eastern part of the Karkonosze Mountains

Reference	Location	Type of material	Lab code	Dating method	Age
Engel *et al.* (2011)	Łomnica Valley	Moraine boulder	Lo-3	^{10}Be exposure-age	19319 ± 506
	Łomnica Valley	Moraine boulder	Lo-4	^{10}Be exposure-age	16782 ± 594
	Łomnica Valley	Moraine boulder	Lo-2	^{10}Be exposure-age	15496 ± 999
	Łomniczka Valley	Moraine boulder	Lk-1	^{10}Be exposure-age	18144 ± 1058
Malkiewicz *et al.* (2016)	Wielki Staw Lake	Plant tissue within lake sediment	Poz-53653	AMS ^{14}C	1004-915*
	Wielki Staw Lake	Plant tissue within lake sediment	Poz-53654	AMS ^{14}C	8422-8315*
	Wielki Staw Lake	Lake sediment	Poz-53655	AMS ^{14}C	11041-10862*

* 2-σ range (^{14}C dating), cal BP

Table 2. General characteristics of the sampling sites

Profile	Latitude	Elevation (m a.s.l.)	Slope inclination (°)	Slope position and shape	Type of rock fragments	Vegetation	WRB (IUSS Working Group 2015)
K1	N 50°45’11,9’’ E 15°47’38,7’’	1269	8	Upper slope (convex)	Mica schist/amphibole schist	*Vaccinio-Piceetea*	Katoskeletic Folic Albic Podzol (Loamic, Densic)
K2	N 50°45’14,3’’ E 15°47’38,5’’	1241	21	Upper slope (straight)	Mica schist/amphibole schist	*Vaccinio-Piceetea*	Endoskeletic Folic Albic Podzol (Loamic)
K3	N 50°45’17,3’’ E 15°47’40,8’’	1198	22	Middle slope (straight)	Mica schist/amphibole schist/gneiss	*Vaccinio-Piceetea*	Endoskeletic Folic Albic Podzol (Loamic)
K4	N 50°45’19,4’’ E 15°47’45,2’’	1178	14	Lower slope (concave)	Mica schist/gneiss	*Vaccinio-Piceetea*	Dystric Endoskeletic Histic Stagnic Cambisol (Loamic, Colluvic)
K5	N 50°45’21,6’’ E 15°47’51,9’’	1145	10	Lower slope (concave)	Mica schist/gneiss	*Vaccinio-Piceetea*	Dystric Folic Stagnosol (Siltic, Endoskeletic, Colluvic)

Table 3. Morphological description of the investigated soil profiles

Soil horizon	Depth (cm)	Colour (moist)	Structure	Consistence (moist)	Boundary	Rock fragments arrangement
K1 - Katoskeletic Folic Albic Podzol (Loamic, Densic)						
Oi	14-6				C, W	
Oe	6-0	7.5YR 2,5/1			C, W	
E	0-22	10YR 6/1	AB, MO	FR	G	V/L
2Bh	22-55	10YR 6/1	SB, WE	FR	C	NO
2Bhs	55-61	5YR 3/3	SB/PL, MO/ST	FI	G	L
3BC	61-80	2.5Y 5/4	PL, MO	VFI	G	L
3C	80-105	2.5Y 5/5	SB, MO	VFI		L
K2 - Endoskeletic Folic Albic Podzol (Loamic)						
Oi	13-7				G, W	
Oe	7-0				C, W	
E	0-12	10YR 5/2	AB, MO	FR	G	NO
2Bhs	12-47	5YR 4/4	SB, WE	FR	G	NO
2Bs	47-63	10YR 5/6	AS, MO	FI	G	L
2BC	63-78	10YR 6/6	AS, MO	VFI	G	L
3C	78-89	10YR 6/8	AS, MO	VFI		L
K3 - Endoskeletic Folic Albic Podzol (Loamic)						
Oi	11-6					
Oa	6-0	10YR 2/1			C, W	
E	0-15	10YR 5/2	AB, MO	FR	C, W	V
2Bh	15-25	5YR 3/2-3	AS, WE	FR	C, W	NO
2Bhs	25-41	7.5YR 4/6	AS, MO	FI	G	L
3BC	41-53	10YR 5/6	SB, MO	FI		L
K4 - Dystric Endoskeletic Histic Stagnic Cambisol (Loamic, Colluvic)						
Oe	10-0	10YR 2/1				
EBg	0-15	7.5YR 4/2	AB, MO	FR	C, W	V
2Bw1	15-30	7.5YR 3/4	SB, WE	FR	G	NO
2Bw2	30-42	10YR 4/4	PL, MO	FR	G	L
3BC	42-63	2.5Y 4/4	AB/PL, MO	FI	G	NO
3C	63-83	2.5Y 4/5	PL/AB, MO	FI		NO
K5 - Dystric Folic Stagnosol (Siltic, Endoskeletic, Colluvic)						
Oi	14-8					
Oa	8-0	10YR 2/1			C, W	
Eg	0-20	10YR 5/2	AB, MO	FR	G	L
EBg	20-38	7,5YR 4-5/4	AB, MO	FR	G	L
2Bwg	38-50	10YR 5/6	AB/PL, MO	FI	G	L
3BC	50-75	10YR 5/8	PL/AB, MO	VFI	G	L
3C	75-95	10YR 5/6-8	AB, MO	VFI		L

Explanations: types of soil structure: AB - angular blocky, AS - angular and subangular blocky, SB - subangular blocky, PL ¬ platy; grade of development: WE - weak, MO - moderate, ST — strong; consistence (moist): FR — friable, FI — firm, VFI — very firm; horizon boundary (distinctness, topography): A - abrupt, C - clear, G - gradual, S - smooth, W – wavy, rock fragments arrangement: V- vertical, L- lateral, NO- no order

able 4. Particle size distribution of the soils.

Soil Horizon	Depth (cm)	Skeleton content	Sand					Silt		Clay fraction	Sum of fractions		Texture class
			vcS	cS	mS	fS	vfS	cSi	fSi		Sand	Silt	
			%										
K1 - Katokeletic Folic Albic Podzol (Loamic, Densic)													
E	0-22	40	1	3	7	31	23	17	12	6	65	29	SL
2Bh	22-55	80	2	9	14	34	21	10	6	4	80	16	LS
2Bhs	55-61	90	7	14	17	26	14	12	6	4	78	18	LS
3BC	61-80	90	3	8	10	25	17	19	12	6	63	31	SL
K2 - Endoskeletic Folic Albic Podzol (Loamic)													
E	0-12	60	3	7	8	24	18	20	14	6	60	34	SL
2Bhs	12-47	70	4	8	14	32	18	12	8	4	76	20	SL
2Bs	47-63	80	8	9	11	26	17	15	10	4	71	25	SL
2BC	63-78	90	7	10	12	27	17	13	10	4	73	23	SL
K3 - Endoskeletic Folic Albic Podzol (Loamic)													
E	0-15	40	2	4	7	27	16	16	22	6	56	38	SL
2Bh	15-25	60	2	9	22	31	17	9	6	4	81	15	LS
2Bhs	25-41	80	3	7	11	27	18	16	12	6	66	28	SL
3BC	41-53	90	8	12	12	21	16	15	12	4	69	27	SL
K4 - Dystric Endoskeletic Histic Stagnic Cambisol (Loamic, Colluvic)													
EBg	0-15	30	5	8	14	23	16	14	14	6	66	28	SL
2Bw1	15-30	40	5	7	18	30	16	10	8	6	76	18	SL
2Bw2	30-42	60	8	11	15	23	13	10	12	8	70	22	SL
3BC	42-63	70	8	11	17	24	12	10	12	6	72	22	SL
K5 - Dystric Folic Stagnosol (Siltic, Endoskeletic, Colluvic)													
Eg	0-20	30	2	2	5	16	13	25	31	6	38	56	SiL
EBg	20-38	50	1	3	5	15	14	23	29	10	38	52	SiL
2Bwg	38-50	40	2	4	6	18	14	21	25	10	44	46	L
3BC	50-75	80	2	3	5	17	17	25	25	6	44	50	L

Table 5. Main soil characteristics

Soil Horizon	Depth	Bd	pH KCl	SOC	EA	BC	BS	Fe_o	Fe_d	Al_o	Al_d	Fe_o/Fe_d	$Al_o+1/2Fe_o$
	cm	g cm^{-3}		%	cmol (+) kg^{-1}			%					%
K1 - Katoskeletic Folic Albic Podzol (Loamic, Densic)													
E	0-22	1.54	2.36	2.98	2.18	1.01	32	0.071	0.086	0.050	0.074	0.83	0.09
2Bh	22-55	1.56	3.01	3.67	8.45	1.00	11	1.768	2.287	0.478	0.512	0.77	1.36
2Bhs	55-61	n.d.	3.65	3.18	4.72	0.74	14	1.520	2.320	0.695	0.752	0.65	1.46
3BC	61-80	n.d.	3.98	0.61	1.45	0.61	30	0.325	1.130	0.418	0.462	0.29	0.58
K2 - Endoskeletic Folic Albic Podzol (Loamic)													
E	0-12	1.54	2.42	5.01	3.28	1.26	28	0.141	0.245	0.075	0.086	0.58	0.15
2Bhs	12-47	1.57	3.31	3.46	6.76	0.92	12	3.100	3.312	0.803	0.915	0.94	2.35
2Bs	47-63	n.d.	4.05	1.31	2.00	0.63	24	0.608	1.204	0.573	0.636	0.50	0.88
2BC	63-78	1.54	4.00	0.93	1.65	0.66	29	0.288	0.965	0.563	0.739	0.29	0.71
K3 - Endoskeletic Folic Albic Podzol (Loamic)													
E	0-15	1.63	2.73	4.99	4.53	0.88	16	0.395	0.640	0.113	0.214	0.62	0.31
2Bh	15-25	1.14	3.10	5.88	8.79	0.93	10	5.350	5.371	0.689	0.764	0.99	3.36
2Bhs	25-41	n.d.	3.66	1.83	3.84	0.77	17	1.848	2.557	0.530	0.611	0.72	1.45
3BC	41-53	1.50	4.03	1.08	1.90	0.60	24	0.503	1.265	0.475	0.498	0.40	0.73
K4 - Dystric Endoskeletic Histic Stagnic Cambisol (Loamic, Colluvic)													
EBg	0-15	0.78	3.69	4.71	8.28	0.63	7	1.718	1.913	0.321	0.388	0.90	1.18
2Bw1	15-30	0.74	3.83	2.09	7.24	0.68	9	1.739	1.986	0.481	0.623	0.88	1.35
2Bw2	30-42	1.21	4.09	0.74	4.68	0.47	9	0.591	0.678	0.279	0.330	0.87	0.57
3BC	42-63	1.21	4.30	0.57	3.24	0.44	12	0.279	0.391	0.296	0.437	0.71	0.44
K5 - Dystric Histic Stagnosol (Siltic, Endoskeletic, Colluvic)													
Eg	0-20	1.87	3.06	5.37	7.01	0.90	11	1.058	1.470	0.260	0.310	0.72	0.79
EBg	20-38	1.25	3.33	3.69	5.60	0.69	11	1.280	1.785	0.278	0.386	0.72	0.92
2Bwg	38-50	1.44	3.60	2.08	4.32	0.82	16	1.203	1.314	0.400	0.492	0.92	1.00
3BC	50-75	1.87	3.77	2.07	3.70	0.70	16	1.325	1.449	0.568	0.638	0.91	1.23

Explanation: Bd – bulk density, SOC – soil organic carbon, EA – exchangeable acidity, BC – base cations (sum), BS – base saturation, Fe_o/Al_o – oxalate extractable Fe/Al, Fe_d/Al_d – dithionite extractable Fe/Al.

Table 6. Total elemental concentrations in the fine earth fractions

Horizon	Depth (cm)	SiO_2	Al_2O_3	Fe_2O_3	K_2O	Na_2O	MgO	CaO	P_2O_5	MnO	TiO_2	Ba	Hf	Zr
		%											mg kg^{-1}	
K1 - Katoskeletic Folic Albic Podzol (Loamic, Densic)														
E	0-22	75.20	12.69	1.23	3.69	2.16	0.56	0.38	0.001	0.036	0.791	829	19.0	709
2Bh	22-55	50.98	12.9	6.68	3.6	2.02	0.84	0.48	0.343	0.046	0.908	758	16.0	478
2Bhs	55-61	50.02	15.3	9.15	3.07	1.61	1.9	1.07	0.255	0.093	1.230	501	12.4	275
3BC	61-80	62.17	14.92	10.61	2.48	2.13	3.21	3.16	0.282	0.144	2.372	346	8.7	348
K2 - Endoskeletic Folic Albic Podzol (Loamic)														
E	0-12	64.01	14.07	1.72	3.71	1.9	0.77	0.33	0.155	0.036	1.015	640	14.9	536
2Bhs	12-47	52.49	14.42	11.26	3.48	2.02	1.54	0.49	0.291	0.076	1.127	596	16.2	346
2Bs	47-63	62.64	13.74	6.17	3.41	1.85	1.41	0.67	0.138	0.086	0.993	606	13.7	434
2BC	63-78	66.08	14.24	5.82	3.42	1.82	1.47	0.71	0.142	0.089	0.983	600	14.7	432
K3 - Endoskeletic Folic Albic Podzol (Loamic)														
E	0-15	65.59	13.31	2.46	3.58	1.48	0.85	0.26	0.129	0.04	1.263	547	14.7	494
2Bh	15-25	47.40	12.56	13.04	2.56	1.39	0.93	0.27	0.374	0.047	1.151	382	8.9	343
2Bhs	25-41	59.52	13.99	7.86	3.22	1.59	1.55	0.42	0.152	0.075	1.056	501	14.0	423
3BC	41-53	63.45	14.14	6.44	3.5	1.6	1.61	0.51	0.14	0.094	1.091	538	15.2	456
K4 - Dystric Endoskeletic Histic Stagnic Cambisol (Loamic, Colluvic)														
EBg	0-15	55.47	13.77	6.19	3.14	1.66	1.31	0.72	0.341	0.046	1.235	436	12.9	374
2Bw1	15-30	56.89	13.37	9.37	2.6	1.4	2.01	1.2	0.114	0.09	1.622	370	11.8	372
2Bw2	30-42	62.62	14.31	8.32	2.95	1.67	2.21	1.32	0.112	0.12	1.713	393	6.9	355
3BC	42-63	63.99	14.34	7.89	3.08	1.57	2.18	1.26	0.133	0.129	1.692	411	7.1	360
K5 - Dystric Folic Stagnosol (Siltic, Endoskeletic, Colluvic)														
Eg	0-20	55.26	15.33	4.59	3.34	1.39	1.42	0.41	0.384	0.028	1.184	430	11.1	398
EBg	20-38	62.90	14.23	4.75	3.27	1.46	1.13	0.49	0.247	0.045	1.247	443	13.1	393
2Bwg	38-50	66.19	14.57	5.68	3.15	1.66	1.42	0.54	0.132	0.058	1.286	426	12.9	391
3BC	50-75	62.08	14.81	5.87	3.13	1.57	1.32	0.5	0.165	0.063	1.248	436	14.1	385

Table 7. ^{10}Be concentrations along the profiles and derivation of erosion rates using two approaches (equation 1 and according to Lal (2001), equation 3).

Profile	Horizon	Depth (cm)	Bulk density (g cm^{-3})	Weight FE[1)] (g cm^{-2})	^{10}Be atoms per g (1E+8)	Soil skeleton (w.-%)	^{10}Be atoms per horizon (1E+8) and cm^{-2}	Erosion rate (t ha^{-2} y^{-1}), eq. 1	Erosion rate (t ha^{-2} y^{-1}), eq. 3	Erosion rate* (t ha^{-2} y^{-1}), eq. 1	Erosion rate* (t ha^{-2} y^{-1}), eq. 3
K1	E	0-22	1.54	33.88	0.08 ±0.00	18	2.19				
	2BH	22-55	1.56	51.48	0.66 ±0.02	68	10.83				
	2BHS	55-61	1.57	9.42	2.83 ±0.05	53	12.53				
	3BC	61-80	1.62	30.78	2.26 ±0.04	39	42.45				
	3C	80-105	1.50	37.50	2.43 ±0.05	46	41.81				
								6.4	10.2	2.0	4.1
K4	EBG	0-15	0.78	11.70	0.85 ±0.03	7	9.28				
	2Bw1	15-30	0.74	11.10	2.07 ±0.05	22	17.94				
	2Bw2	30-42	1.21	14.52	3.04 ±0.07	36	28.28				
	3BC	42-63	1.21	25.41	2.96 ±0.04	39	45.87				
	3C	63-83	1.50	30.00	1.47 ±0.05	41	26.10				
								1.3	1.3	0.8	0.7
K5	EG	0-20	1.87	37.40	0.65 ±0.02	10	21.93				
	EBG	20-38	1.25	22.50	0.64 ±0.02	32	9.81				
	2BWG	38-50	1.44	17.28	1.69 ±0.04	36	18.64				
	3BC	50-75	1.87	46.75	2.38 ±0.04	58	46.71				
	3C	75-95	1.52	30.40	1.47 ±0.05	57	19.03				
								1.7	2.9	1.6	2.2

[1)] FE = FINE EARTH

* SCENARIO WHEN NOT CONSIDERING THE UPPERMOST HORIZON (THAT MOST LIKELY HAS A DIFFERENT ORIGIN WHEN COMPARED TO THE UNDERLYING SOIL)

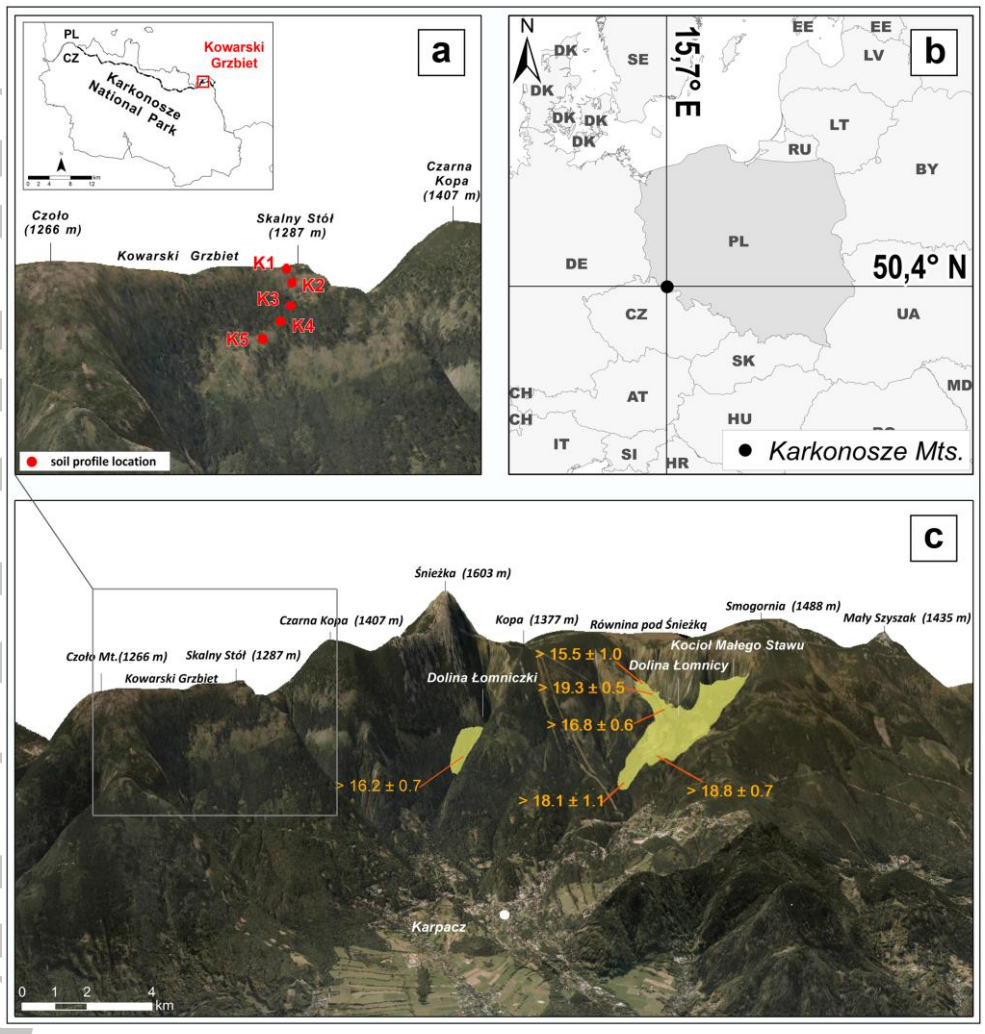

Fig. 1. General location of the Karkonosze Mts. (b) and sampling sites with individual position of the soil profiles (a) and topographic situation (c) of the western part of the mountain range including the ages of moraines (based on Engel et al., 2014).

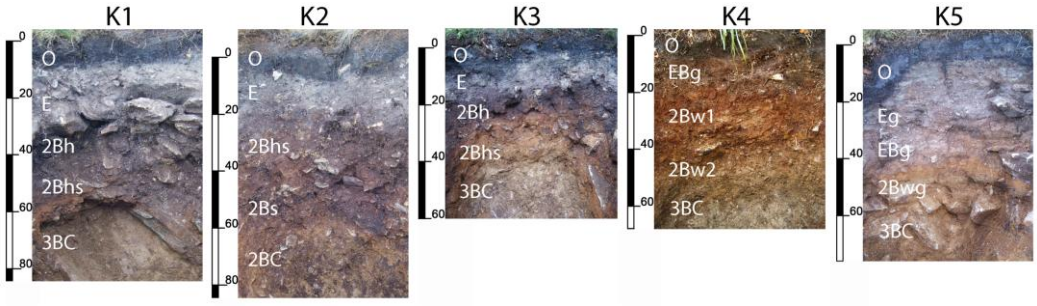

Fig. 2. Photographs of the soil profiles along the toposequence of the Kowarski Grzbiet (Karkonosze Mts).

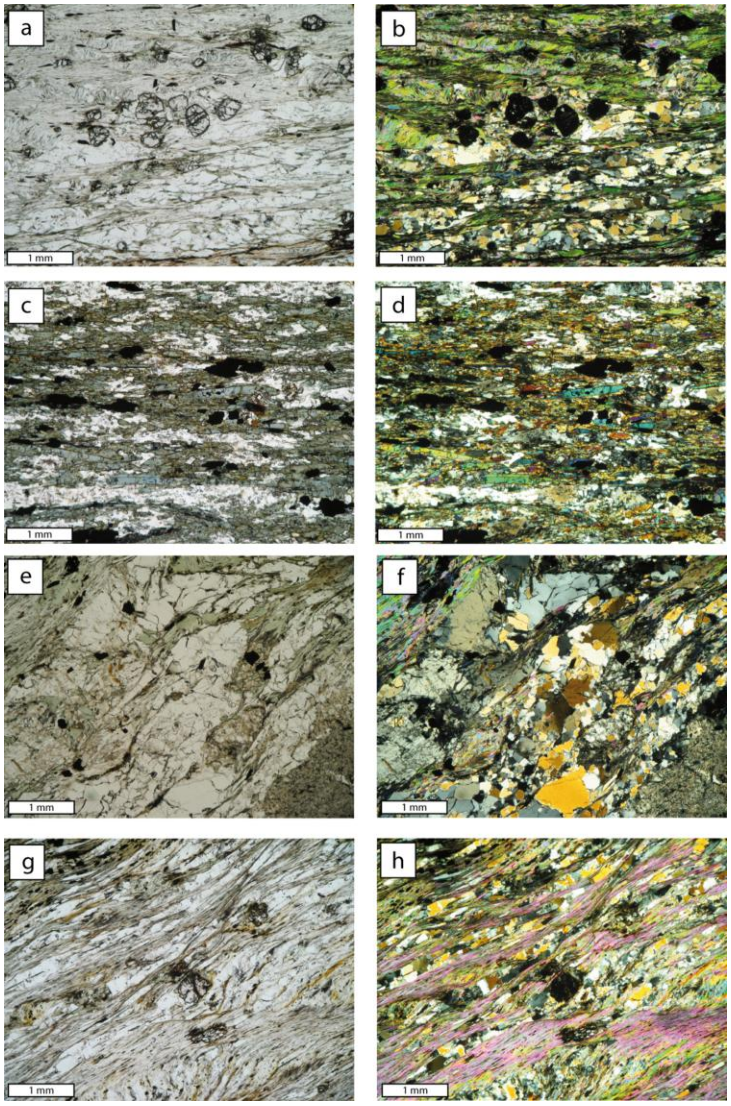

Fig. 3. Microphotographs of the rock fragments in the soil profiles: (a,b) garnet mica schist from the E horizon of the profile K1; (c,d) amphibole schist from the 3BC horizon of profile K1; (e,f) mica schist from the EBg horizon of profile K5; (g,h) gneiss from the 3BC horizon of the profile K5.

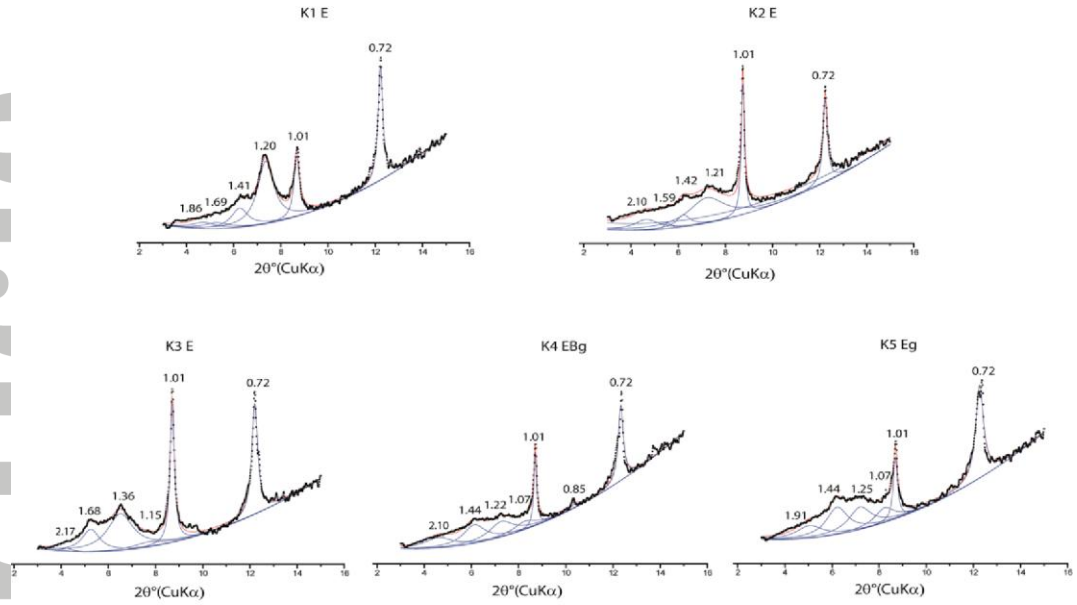

Fig. 4. XRD patterns of the EG-solvated clay fraction from the topsoils along the toposequence. The measured values (squares), modelled elementary curves and the modelled overall curve are shown. The XRD curves are corrected for Lorentz and polarization factors; *d*-spacing in nm.

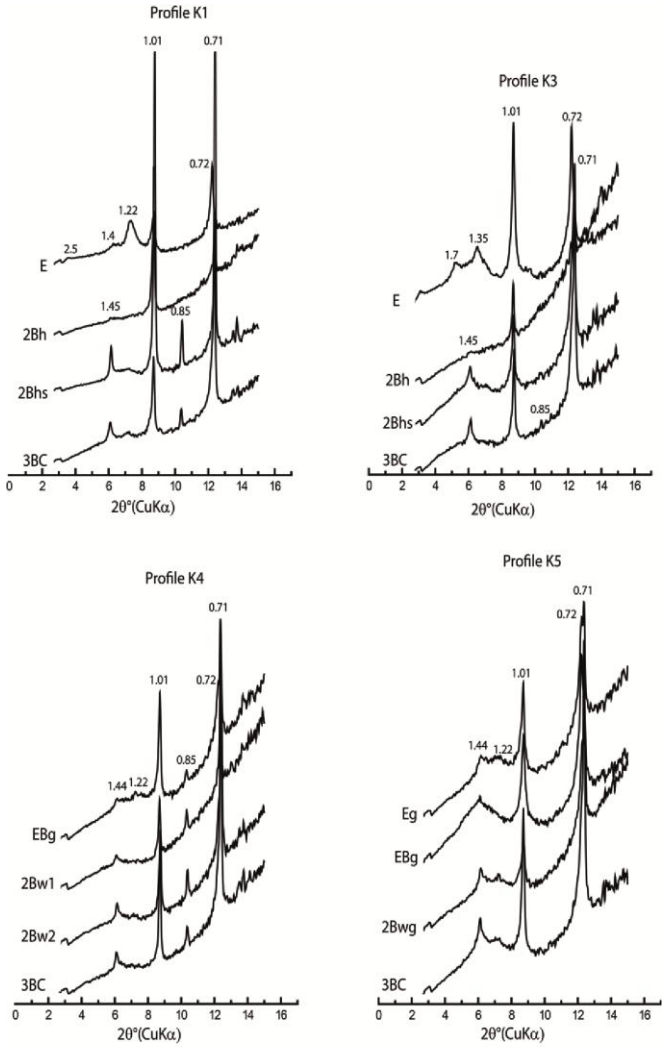

Fig. 5. XRD patterns of soil clays after EG-solvation of all profiles and horizons along the soil catena. The XRD curves are corrected for Lorentz and polarization factors; *d*-spacing in nm.

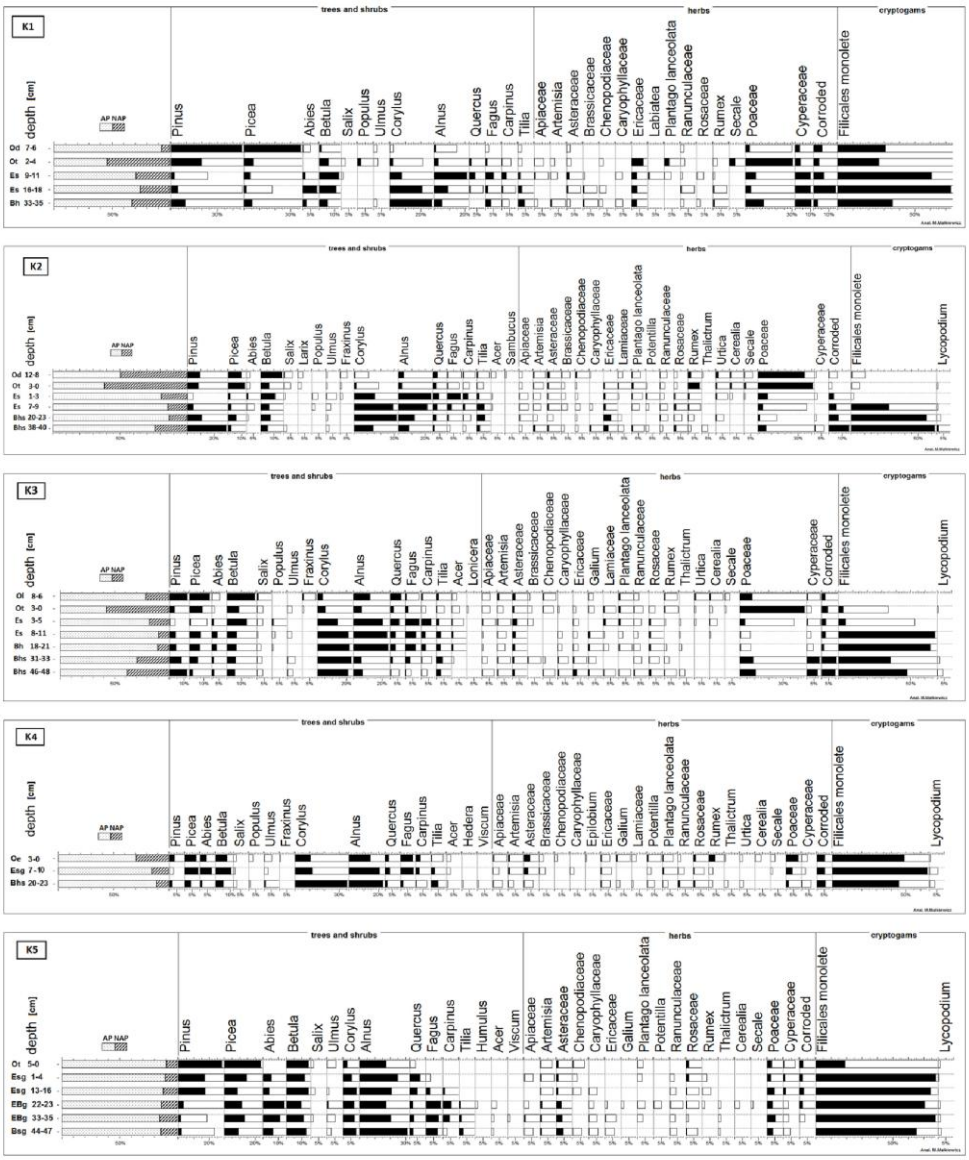

Fig. 6. Pollen diagrams of the studied soil profiles.

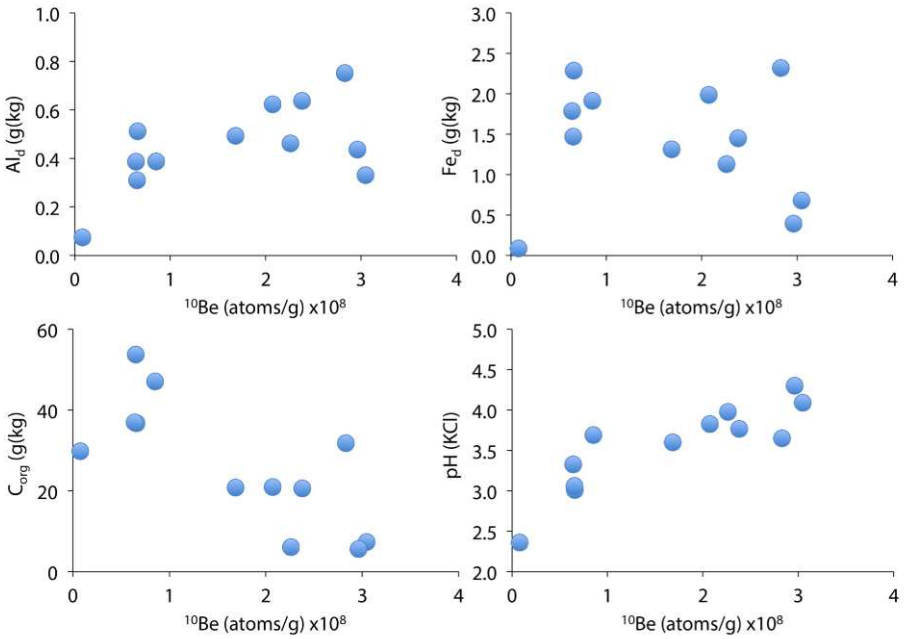

Fig. 7. ^{10}Be concentration in relation to explanatory variables such as the dithionite-extractable Fe and Al, organic carbon and pH.

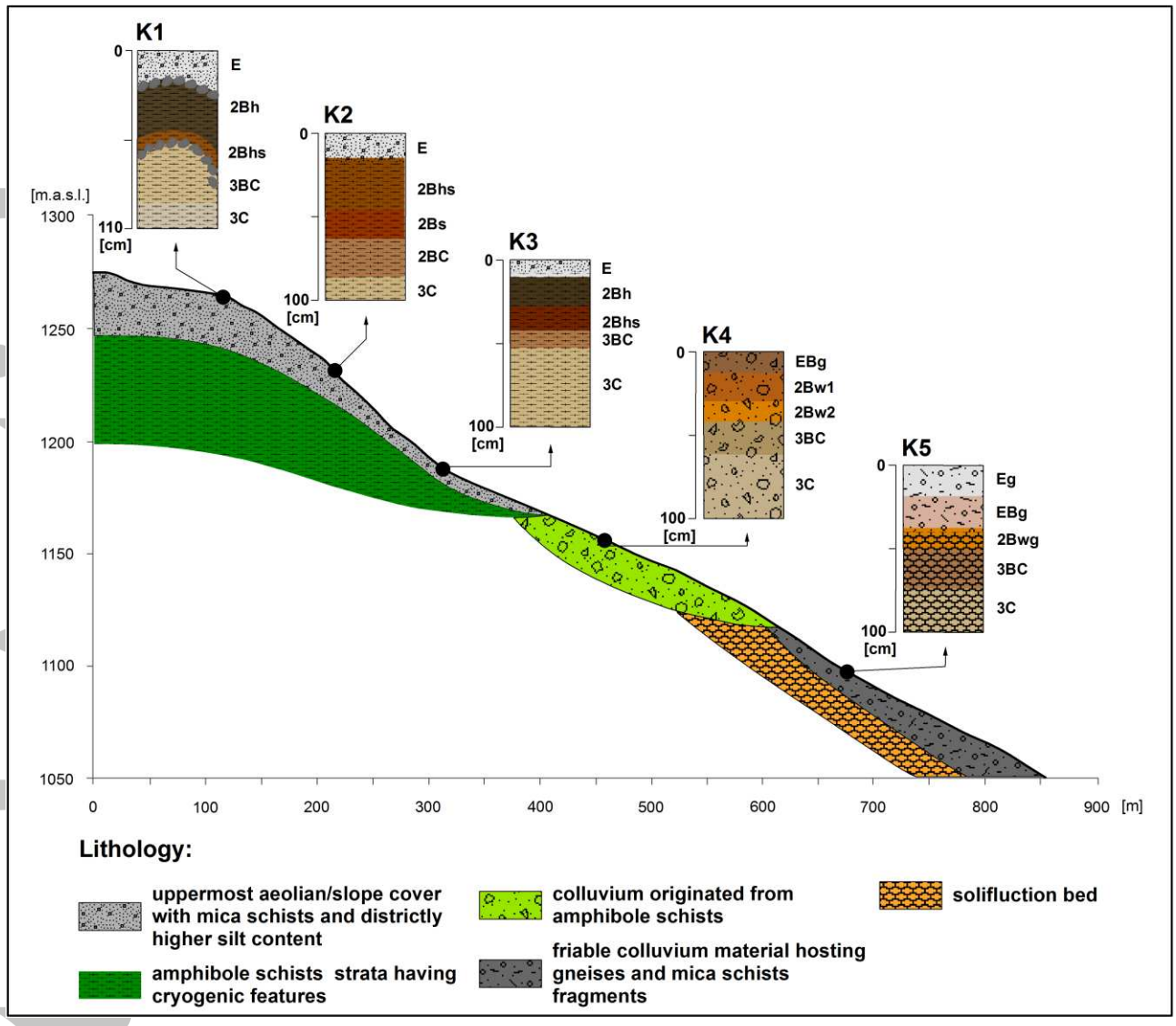

Fig. 8. Scheme of hypothetical arrangement of slope materials along the investigated catena. The thickness of the individual lithological layers and soils are enlarged in the figure.

Identifying slope processes over time and their imprint in soils of medium-high mountains of Central Europe (the Karkonosze Mountains, Poland)

Jaroslaw Waroszewski[a], Markus Egli[b], Dagmar Brandová[b], Marcus Christl[c], Cezary Kabala[a], Malgorzata Malkiewicz[d], Jakub Kierczak[e], Bartłomiej Glina[f], Paweł Jezierski[a]

The applied multidisciplinary approach (palynological, mineralogical and soil chemical analyses, analysis of cosmogenic nuclides) confirmed our hypothesis and clearly demonstrated that soil and landscape evolutuion in the Karkonosze Mountains has been complex. The different strata detected in the soils have either an aeolian origin or are related to mass wasting. Together with the pollen assemblage, timings for the progressive and regressive soil forming phases could be proposed.